Getting Beyond the Bankfull Shields Parameter: A Continuum of Threshold Channel Types Illustrated by the Case of the White Clay Creek, PA

Sophie Bodek[1], James E. Pizzuto[1], Kristen M. McCarthy[1*], Raphael Affinito[1†]

[1]Department of Earth Sciences, University of Delaware, Newark, Delaware, USA 19716

Key Points:

- Bankfull Shields stresses slightly exceed mobility thresholds, but tagged tracers demonstrate that 8–73% of the bed is immobile
- Geomorphic maps indicate that immobile clasts are derived from local colluvium and bedrock
- These are threshold alluvial-colluvial-bedrock rivers with widths likely scaled by cohesive bank erosion thresholds

*EA Science, Engineering, and Technology, Inc., PBC, Hunt Valley, Maryland, USA 21031
†Department of Geosciences, Pennsylvania State University, University Park, Pennsylvania, USA 16802

Corresponding author: Sophie Bodek, sbodek@udel.edu

Abstract

The Shields parameter based on median grain size (D_{50}) and bankfull depth is often used to interpret river morphology, but it may not always be a useful index of sediment transport processes. At 12 sites of the White Clay Creek (WCC), PA, the ratio of bankfull Shields stress to threshold Shields stress averages 1.41 (range 0.41–2.63), suggesting that these channels are alluvial near-threshold gravel-bed rivers. However, field mapping indicates confinement by bedrock and colluvium, and a channel slope dominated by bedrock incision and knickpoint migration. A numerical model of WCC bed material transport and grain size, calibrated to bedload tracer data, demonstrates that 22% (range 8–73%) of the bed material is composed of a population of immobile cobble and boulder-sized sediment supplied through local colluvial processes and bedrock erosion, and a separate population of mobile sand, pebble- and cobble-sized alluvium. Computations also suggest that channel morphology is only weakly coupled to upstream sediment supply. Additional analyses further imply that width adjustment may reflect a balance between cohesive bank erosion and floodplain deposition, though channels nonetheless may be closely scaled by cohesive bank erosion thresholds. WCC represents an example of a continuum of underappreciated, but relatively common, threshold alluvial-colluvial-bedrock rivers with partially immobile beds and widths scaled by cohesive bank erosion thresholds. Fluvial geomorphologists will need to look beyond simple sediment transport metrics to fully understand and classify these stream channels.

Plain Language Summary

Rivers assume various forms and are often classified according to bed material: gravel-bed and sand-bed channels are bounded by sediments that were previously transported by the river, and are sensitive to changes in sediment supply; colluvial-bedrock channels are bounded by material supplied from the surrounding hillslopes or bedrock, and are insensitive to variations in sediment supplied by the river. Despite unique characteristics, these channel types are all influenced by erosion thresholds and are considered threshold channels. Observations of 12 sites at the White Clay Creek (WCC), PA show characteristics that span the aforementioned gravel-bed and colluvial-bedrock channel types. Initially, sediment transport metrics suggest that WCC is a threshold gravel-bed river. Alternately, field surveys show the presence of bedrock and colluvium along channel banks and a population of immobile bed material, while numerical modeling indicates that WCC sites are insensitive to changes in sediment supply–all characteristics of colluvial-bedrock rivers. These observations lead us to classify WCC as an alternate category called the alluvial-colluvial-bedrock river. Here, bed material consists of immobile, locally supplied cobbles and boulders and mobile sediments transported from upstream. Our results suggest that careful observation and measurement of sediment transport are needed to fully understand and classify river channels.

1 Introduction

Alluvial rivers sculpt their channels from sediment transported and deposited by the stream itself. In recent years, the reach-scale morphology of alluvial channels has been interpreted in terms of sediment transport processes reflected by the Shields parameter (Church, 2006; Dade & Friend, 1998; Parker, 1978), which is most often defined using the bankfull depth, D, channel slope, S, and median grain size of the bed material, D_{50}, as $DS/(1.65D_{50})$, where the value of 1.65 assumes quartz bed sediment and a water density of 1000 kg/m^3. For example, gravel-bed rivers with mobile, alluvially supplied bed material often display bankfull Shields stresses slightly in excess of the threshold of motion (Andrews, 1984; Parker, 1978; Phillips & Jerolmack, 2019), while alluvial sand-bed streams have Shields stresses that exceed the threshold of motion by an order of magnitude or more (Church, 2006; Dade & Friend, 1998; Dunne & Jerolmack, 2018).

The clustering of bankfull Shields stresses of alluvial gravel-bed and sand-bed channels has been interpreted to arise from an adjustment of alluvial channel morphology to ensure the transport of the water and sediment supplied from upstream, a manifestation of the concept of graded stream equilibrium (Mackin, 1948). A foundation of these ideas is the necessity of stable banks for the existence of an equilibrium morphology. For gravel-bed rivers, gravel at the toe of the bank is considered to be poised at the threshold of entrainment, thereby ensuring the mobility of gravel bed material, as Shields stresses on the channel bed can then exceed the threshold of motion at bankfull stage, though only by a small amount (Parker, 1978; Vigilar & Diplas, 1997). For sand-bed channels, it has recently been proposed that width is controlled by the threshold of erosion for cohesive bank material (Dunne & Jerolmack, 2018). Sand-bed channels are envisioned to widen until stresses on the bank just equal the threshold of motion, with slope and depth then adjusted to ensure that the river can transport the water and sediment supplied by the watershed. The high erosion resistance of fine-grained cohesive sediment (often enhanced by vegetation) results in high banks, which, along with the small-grain size of sandy bed material, results in bankfull Shields stresses an order of magnitude higher than those of gravel-bed streams.

These hypotheses explain the morphology of alluvial channels in terms of two unifying characteristics. One involves adjustment of morphology to achieve stable threshold banks, while the other involves adjustment to maintain the continuity of water and sediment. Sediment grain size is an independent variable, imposed by upstream transport, while the reach-scale morphology is adjusted by the river through erosion and deposition.

The bankfull Shields parameter and threshold erosion concepts have also provided a foundation for interpreting fluvial processes in some colluvial and bedrock channels. Some coarse-grained rivers have bankfull Shields parameter values essentially at the threshold of motion with minimal bedload transport, except for much finer sediment that is carried downstream as throughput load without influencing channel form. These are often interpreted as colluvial channels, with sediment supplied locally by hillslope processes, slopes imposed by bedrock erosion and other non-alluvial processes, and channel cross-sections sculpted by flow to achieve threshold stresses for entrainment across the entire channel perimeter (Diplas & Vigilar, 1992; Glover & Florey, 1951; Li et al., 1976). The grain size of the colluvial channel perimeter is supplied locally, and is independent of fluvial processes. Bedrock channels mantled by coarse-grained alluvium may also exhibit bankfull Shields numbers close to threshold values, and it appears that episodic mobility of gravel and its supply can significantly influence bedrock erosion and bedrock channel morphology (Johnson et al., 2009).

While each of the stream types described above has unique characteristics, their morphologies are all strongly influenced by erosion thresholds, and therefore they can all be considered different categories of threshold stream channels (Table 1). Each of the different threshold stream types in Table 1 represents an end-member with unique sediment properties and characteristic sediment transport processes, with the Shields parameter providing a useful metric for distinguishing between them.

While the classification in Table 1 is supported by extensive research, our preliminary field observations suggested that the three categories may be too limited, and that the Shields parameter as a means of classification could prove misleading. For example, we hypothesized that typical stream channels of the mid-Atlantic region represent an underappreciated category of alluvial-colluvial-bedrock threshold channel, with a slope and bed architecture imposed by immobile cobbles and boulders derived locally through erosion of colluvium and bedrock, and a width most strongly influenced by erosional processes of cohesive bank sediments. We also observed a bed that appeared to be partly mantled by mobile alluvium, so bankfull Shields stresses are not far above thresholds of motion, similar to those of alluvial gravel-bed rivers. This provides the misleading view

Table 1. Classification of Threshold River Channels

Threshold river type	Bed material mobility at bankfull stage	Bankfull Shields parameter	Bed material sources	Key bank processes	Key references
Alluvial near-threshold gravel-bed	Fully mobile	Slightly > Critical	Supplied from upstream	Gravel at bank toe at threshold of motion	Parker (1978)
Alluvial sand-bed	Fully mobile	≫ Critical	Supplied from upstream	Cohesive bank sediments at threshold of motion	Dunne and Jerolmack (2018)
Colluvial-bedrock	At threshold of motion	Critical	Supplied locally	Cobbles, boulders at threshold of motion	Glover and Florey (1951); Li et al. (1976)
Alluvial-colluvial-bedrock	Only partially mobile	Slightly > Critical	Immobile fraction supplied locally; mobile fraction supplied from upstream	Migrating channels with eroding banks close to cohesive erosion thresholds	This study

that the stream bed is fully mobile at bankfull stage and that gravel stability plays a role in width adjustment.

The study described here presents an analysis of fluvial processes and morphology designed to test these hypotheses. We observed event-scale bedload transport processes and document the geomorphic setting, morphology, and stratigraphy of river reaches throughout the watershed. We use a numerical model of bedload transport, calibrated to local conditions, to assess the mobility of individual grain size fractions and to determine the sensitivity of channel morphology to the supply of bed material. These data motivate us to propose a new, but arguably common, category of threshold river behavior that we term the *alluvial-colluvial-bedrock threshold channel* (Table 1).

2 Study Area

The White Clay Creek watershed covers 279.2 km^2 in southeastern Pennsylvania and northern Delaware (Figure 1a). Land uses are classified as developed (38%), agriculture (32%), forest (28%), and wetlands (2%) (Kauffman & Belden, 2010). The region has a modified humid continental climate with moderately cold winters and warm, humid summers. Water discharge and other data are collected at four U.S. Geological Survey (USGS) stream gages; data from the stream gage near Strickersville, PA (USGS gaging station #01478245) is particularly important for this study.

The White Clay Creek watershed encompasses two physiographic provinces. The northern portion of the watershed lies within the Piedmont Physiographic Province (Fischer et al., 2004; Renner, 1927), which is underlain by late Proterozoic and early Paleozoic metamorphic rocks (Schenck et al., 2000). Near Newark, the White Clay Creek encoun-

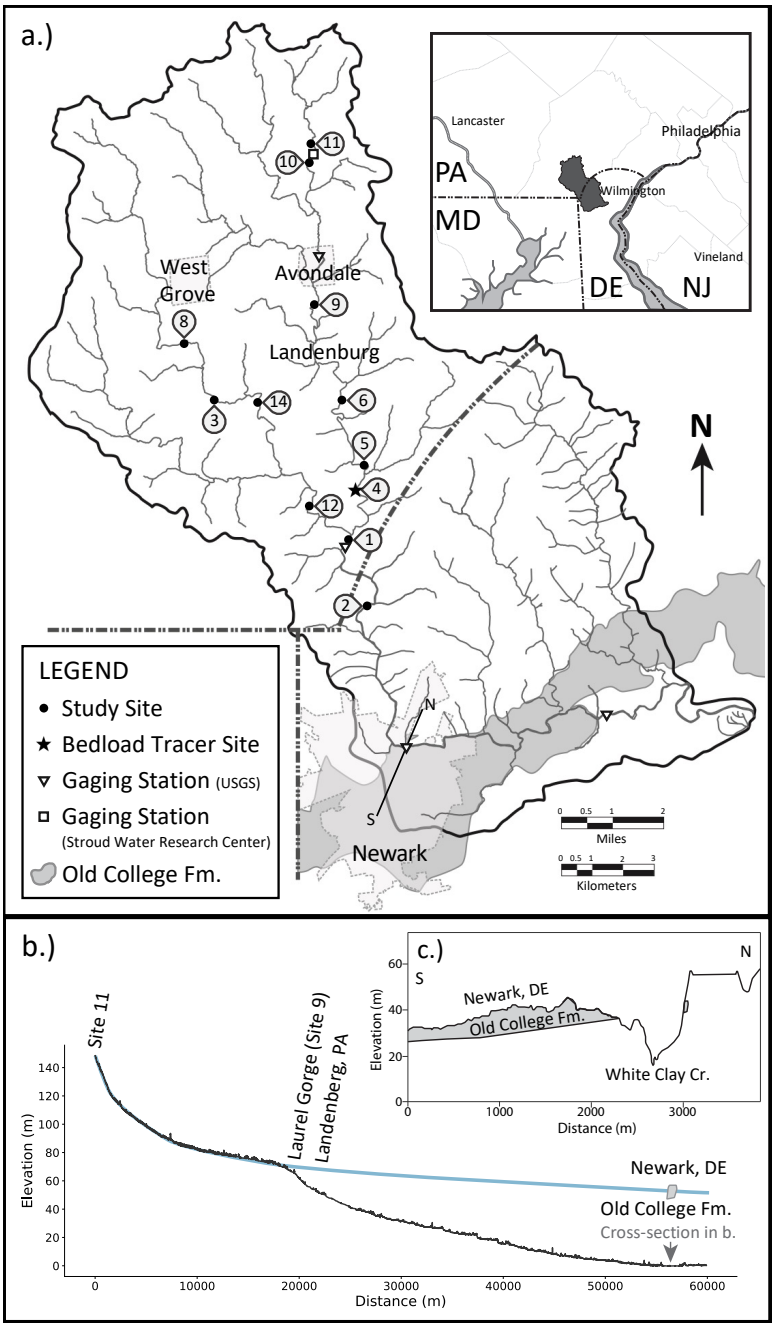

Figure 1. Location, setting, and longitudinal profile of the White Clay Creek. (a) Map of the White Clay Creek watershed showing the locations of 12 study sites, including the bedload tracer study site that was established at Site 4, and the locations of stream gaging stations. The USGS stream gage near Strickerville is just downstream of Site 1. Also indicated is the extent of the Old College Formation and the line of cross-section of Figure 1c. Inset indicates the regional location of the White Clay Creek watershed. (b) Longitudinal profile of the East Branch of the White Clay Creek from Site 11 to Newark, DE. The profile of the ancestral White Clay Creek, shown in light blue, runs through the Old College Formation, an alluvial fan deposit. (c) Cross-section of the White Clay Creek in Newark, DE, showing the extent of the Old College Formation.

ters the Fall Zone, which represents the boundary between the Piedmont Province to the north and the Coastal Plain Physiographic Province to the south. Here the White Clay Creek abruptly turns to the east and encounters Cenozoic sedimentary rocks (Plank et al., 2000; Ramsey, 2005), including the Old College Formation, a 1 Ma-old alluvial fan deposited by a Pleistocene precursor to the modern White Clay Creek (Figure 1).

Fluvial geomorphologists have long recognized the Fall Zone as an important regional control on fluvial morphology in the mid-Atlantic region. As streams approach the Fall Zone, longitudinal profiles steepen and valleys narrow, frequently developing pronounced bedrock gorges (Hack, 1982; Reed, 1981). The Fall Zone has been alternatively interpreted as a hinge point for ongoing Cenozoic crustal warping (Hack, 1982; Pazzaglia, 1993), a locus of crustal movements related to the migration of the Pleistocene glacial forebulge (Pico et al., 2019), or an area of focused incision initiated by meltwater from downwasting Pleistocene ice sheets (Reusser et al., 2004).

3 Methods

Previous studies and preliminary observations lead to the development of an initial conceptual model of the White Clay Creek (Figure 2). Channels are primarily single-thread and sinuous rather than meandering, though they may locally exhibit side channels and mid-channel bars. The channel is often confined by bedrock exposures and colluvium. Floodplains, consisting of cohesive sand, silt, and clay, have been strongly influenced by colonial and more recent watershed disturbances. Grain sizes exposed on the streambed range from sand to boulders; cobbles, pebbles, and sand appear to be supplied through sediment transport from upstream, while boulders and cobbles are sourced locally from colluvium and exposed bedrock. Eroding streambanks are common, supplying sediment ranging from clay to cobble-sized gravel. Mobile bed material is stored in lateral bars, and, to a lesser extent, on a coarse-grained bed that appears to be partly anchored by immobile cobbles and boulders. Sediment stored in bars appears to be mobilized at bankfull stage, while the largest grains on the bed appear to be immobile at bankfull stage.

This conceptual model provides several hypotheses that we test with field observations and model computations. Exposures of bedrock and colluvium and the presence of large immobile clasts on the streambed suggest that the White Clay Creek is not a fully alluvial channel, but should rather be considered a mixed bedrock-alluvial channel. Furthermore, if the supplied gravel bed material mostly behaves as throughput load, then channel morphology should be insensitive to changes in the supply of bed material. Additionally, changes in bed material supply should be readily accommodated by changes in the grain size of stored bed material, rather than changing morphology, as would be expected for alluvial channels.

Field observations across multiple scales and bedload transport computations provide data to test and refine our preliminary conceptual model for the White Clay Creek. A longitudinal profile of the entire watershed is used to assess relationships between fluvial processes and the White Clay Creeks underlying bedrock. Studies of reach-scale stream morphology and grain size over a range of stream orders provide estimates of bankfull Shields stresses across the watershed. Geomorphic mapping, stratigraphic analyses, and measurements of bank erosion rates provide additional data. To more precisely assess the mobility of sediments of varying sizes, radiotracers were installed in bed sediments at one site and tracked over 4 significant storm events. These data were used to calibrate an equation for the motion of individual bedload grain size fractions. Once calibrated, this equation was used to assess the mobility of different grain sizes at our field sites at bankfull stage, and to better understand the relationship between bed mobility and bankfull Shields parameter values. The calibrated bedload transport model was also used to

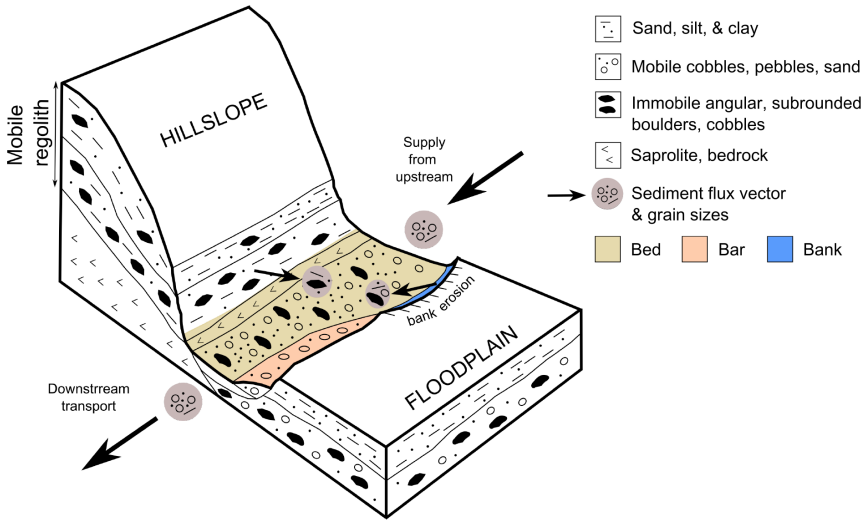

Figure 2. Preliminary conceptual model of bed material supply and flux in the White Clay Creek. Immobile cobbles and boulders are supplied locally through bank erosion and channel incision, while the fluvial supply from upstream consists of sand and pebbles stored in bars. The streambed is anchored by cobbles and boulders that are immobile at bankfull stage, but contains a sparse covering of throughput load consisting of sand and pebbles primarily supplied from upstream (but augmented by locally eroding banks).

188 determine the sensitivity of the channel of the White Clay Creek to changes in the sup-
189 ply of bed material.

190 3.1 Longitudinal profile

191 Watershed scale geologic controls on channel morphology were documented by cre-
192 ating a longitudinal profile. Channel centerlines were first hand-drawn in an ArcGIS en-
193 vironment from high-resolution aerial imagery. Centerlines were extended upstream un-
194 til the channel could no longer be clearly identified. Elevations along the centerline were
195 then extracted from a Digital Elevation Model created from aerial LiDAR survey data.

196 3.2 Documenting reach-scale fluvial morphology

197 Twelve sites were selected to document reach-scale characteristics of the White Clay
198 Creek (Figure 1a, Table 2). All of the sites are within the Piedmont Physiographic Province
199 and all except one are located in Pennsylvania; the lone site in Delaware is about 1 km
200 downstream of the Pennsylvania border. Study reaches varied from 157 to 811 m in length;
201 riparian zones were both forested and in pasture (Table 2). Five of the sites have side
202 channels or well-developed mid-channel bars, while the remainder are single-thread chan-
203 nels. Most of the sites are sinuous (sinuosity < 1.5), but two sites have sinuosities in ex-
204 cess of 1.5 and could be considered meandering (Table 2). Bedrock and colluvium bor-
205 der the channel at 9 of the 12 sites, and eroding banks are pervasive. Five sites are in-
206 fluenced by engineering structures, including abandoned railroads, and at one site, his-
207 toric rip-rap along one of the banks. Some sites have breached or extant colonial mill
208 dams within 0.4–2.1 km either upstream or downstream.

209 Survey and grain size data documented the morphology and bed and bar grain size
210 distributions at the 12 sites. One cross-section was surveyed at a representative location

of each site, except at Site 4 (the site of the bedload tracer study), where three cross-sections were surveyed. Longitudinal profiles documented slopes of the water surface and streambed along the channel centerline. The grain size distribution of the bed and bar material at each study site was determined using the Wolman (1954) method; at least 100 clasts were sampled from both the surface of the streambed and a typical bar, resulting in a minimum error of 20% on individual grain size percentiles (Rice & Church, 1996).

Geomorphic maps were created to document each sites geomorphic setting. Mapped features included exposures of bedrock and colluvium, large boulders, anthropogenic structures (e.g., old railroad grades, rip rap, etc.), large wood, riparian vegetation, pools and riffles, locations of tributaries, side channels, eroding banks, and various types of bars.

The stratigraphic setting was documented through measurements and observations of deposits exposed in eroding banks, and also by creating a geologic cross-section at Site 1. Deposits were classified visually and interpreted in the context of previous studies of valley-fill sediments of the mid-Atlantic region (Jacobson & Coleman, 1986; Walter & Merritts, 2008). At Site 1, sediments were sampled using a bucket auger along a surveyed topographic cross-section.

Decadal average rates of eroding bank retreat were measured at each site. Erosion rates were measured using a combination of repeat historical aerial imagery (Rhoades et al., 2009) and dendrochronology (Stotts et al., 2014). Detailed discussion of methods and results are presented by McCarthy (2018).

3.3 Bedload tracer study

Bedload tracer particles were installed during the summer of 2019 at a 100 m reach at Site 4, which is located approximately 2.8 km upstream of the Strickersville gaging station (Figure 1a). Tracer particles consisted of 32 mm HDX (half duplex) RFID (radio frequency identification) tags manufactured by Oregon RFID. The tags were placed at random locations throughout the reach and were attached to a wide range of sediment sizes. The first RFID tags were installed in June through early July 2019 and the grain size distribution of the tagged clasts mirrored the grain size distribution of the bed. Additional clasts were tagged in late July 2019 and in October 2019, resulting in a total of 56 tagged clasts ranging in size from 1 cm to 144 cm.

The tracers were installed in situ on the streambed by drilling holes into clasts that were exposed above the surface of the water at low flow. The RFID tags were placed in the holes and sealed in place with a waterproof epoxy. Tags were installed in situ wherever possible in order to prevent our actions from disturbing the bed and increasing the likelihood of transport. In order to tag clasts that were underwater, the waterproof epoxy was used as a glue to attach a tag to the surface of each clast. If clasts were sufficiently small (1–5 cm), the tag could not be affixed without disturbing the bed. These small clasts were removed from the streambed in order to attach the RFID tag.

After installation, tagged particles were surveyed at regular intervals. Surveys occurred weekly during July 2019 with subsequent surveys occurring monthly from August 2019 to January 2020. A total of nine surveys were completed over the course of the study (not including the initial survey that first established clast location). For all surveys, the RFID tags were located using an antenna reader manufactured by Oregon RFID with a 0.5 m detection radius. Once a tagged clast was found, its location was recorded using an electronic total station located above a benchmark on a gravel bar. Since the detection radius of the RFID reader antenna is 0.5 m (Phillips & Jerolmack, 2014), the detection threshold was set to the same value, with all tracer motion below 0.5 m considered as error and set to zero. Tracer recovery ranged from 100–66%. The recovery rate of the final survey, which occurred in January 2020, was unusually low (66%) due to the

Table 2. Location and Geomorphic Setting of 12 Study Sites

Site no.	Location	Stream order	Reach length	Sinuosity	Fraction[a] exposed bedrock and colluvium	Fraction[a] with at least 1 eroding bank	Riparian vegetation[b] of outer bank	Side channels or mid-channel bars present	Fraction[a] influenced by anthropogenic structures	Type of structure[c]	Distance, direction[d] to nearest mill dam[e]
	[°N, °W]	[–]	[m]	[–]	[–]	[–]	[–]	[–]	[–]	[–]	[km]
1	39°44'55.16", 75°46'11.67"	4	157	1.04	0	0.81	Forest	No	0.17	Bridge, RR	1.3, ds, B
2	39°43'44.70", 75°45'40.16"	4	198	1.74	0	1	Pasture	Yes	0	none	1, us, E
3	39°47'11.44", 75°49'8.24"	2	316	1.22	0.12	0.66	Pasture	Yes	0	none	none
4	39°45'47.48, 75°45'59.61"	3	170	1.27	0.34	0.48	Forest	Yes	0.18	RR	2.1, us, E
5	39°46'6.56", 75°45'46.58"	3	184	1.36	0.25	0.49	Pasture	No	0	none	1.2, us, E
6	39°47'5.57", 75°46'27.45"	3	811	1.09	0.79	0.25	Forest	No	0.36	RR, BCMD	0.5, ds, B
8	39°48'12.96", 75°49'47.63"	2	326	1.05	0.09	0.49	Pasture	Yes	0.08	ECMD	0.4, ds, E
9	39°48'47.07", 75°47'4.64"	3	214	1.79	0	0.74	Forest	No	0	none	1.8, ds, B
10	39°51'21.32", 75°47'1.28"	2	678	1.43	0.06	0.85	Pasture	No	0	none	none
11	39°51'40.61", 75°47'2.51"	2	610	1.12	0.30	0.76	Forest	No	0	none	none
12	39°45'19.89", 75°47'8.33"	3	504	1.36	0.59	0.31	Forest	Yes	0.17	riprap	1.3, ds, E
14	39°47'9.31", 75°48'10.98"	2	514	1.02	0.51	0.86	Forest	No	0	none	none

[a]Fractions are by reach length. [b]Forested—tree density > 0.3 trees/m^2, see McCarthy (2018) for details. [c]RR—railroad, BCMD—breached colonial mill dam, EMCD—extant colonial mill dam, riprap—historic bank stabilization by boulders. [d]ds—downstream, us—upstream. [e]B—breached, E—extant.

occurrence of a flow event that nearly reached bankfull stage. It is likely that several tagged clasts were transported out of the study reach, or onto the bar or banks where they were not detected.

The water level in the reach was surveyed for two significant flow events on 27 October 2019 and 25 January 2020. Within 3 days after each event, the high water marks on both sides of the channel were flagged based on observations of disturbed leaves, flattened vegetation, or debris left along the bank. Later, the flagged high water marks were surveyed using an electronic total station or automatic level. The location of each tagged clast was also recorded during these surveys. The difference in height between the tracer and nearest high water mark was utilized to determine the depth of water above that clast.

3.4 Calibrating a bedload transport model

To assess bedload transport at the various study reaches, we use the sediment transport model developed by Wilcock and Crowe (2003) that determines the transport rate for mixed sediment sizes, including sand. This model is chosen due to the utilization of the full grain size distribution of the bed surface and its wide applicability.

Bedload tracer data are used to calibrate the sediment transport model for conditions at the White Clay Creek. Similar to many other sediment transport equations, the Wilcock and Crowe (2003) sediment transport model requires a reference shear stress (τ_{*ri} or τ_{ri}) (e.g., Parker, 1990; Parker & Klingeman, 1982; Parker et al., 1982; Wilcock, 2001), defined as the Shields stress (τ_*) or shear stress (τ) at which a dimensionless transport parameter is equal to a reference value (Parker et al., 1982). This reference value ($W_{*r} = 0.002$) represents a threshold of motion, where sediment sizes with a dimensionless transport parameter less than the reference value ($W_{*i} < 0.002$) are considered immobile (Parker et al., 1982).

While the value of the reference shear stress can be determined using a variety of approaches (e.g., Parker et al., 1982; Segura & Pitlick, 2015; Wilcock & Crowe, 2003), the data collected in this study are poorly suited to previous methods. Here we define the reference shear stress (τ_{ri}) for a particular particle as the stress that is associated with a transport distance of a single grain diameter.

The shear stress generated by each flow event was determined by correlating the measured depth in the study reach (determined by the high water mark surveys and cross-sectional surveys) to the gage height at the downstream Strickersville gage. It is assumed that the highest flow event prior to each survey was responsible for mobilizing all bedload tracers. By relating the shear stress of the flow events to bedload tracer mobility, a range of reference shear stresses for each grain size category (τ_{ri}) could be determined. A relationship between grain size and average reference shear stress could then be ascertained for all grain sizes, even those too small to tag or too large to be mobilized by conditions observed during the study period. Thus, two important parameters were found—the reference shear stress for the mean grain size (τ_{rm}) and the hiding function exponent (b), which are utilized in the following hiding function:

$$\tau_{ri} = \tau_{rm} \left(\frac{D_i}{D_m} \right)^b \tag{1}$$

where τ_{rm} is the reference shear stress for the geometric mean grain size (D_m), τ_{ri} is the reference shear stress for a given grain size (D_i), and b is the hiding function exponent. The range of reference shear stresses, τ_{ri}, and the magnitude of b has been observed to vary in different environments (e.g., Andrews & Parker, 1987; Kuhnle, 1993; Parker et al., 1982; Wilcock, 1993), necessitating field-based observations when determining these values.

Due to the range of reference shear stresses found for each grain size category, a 5% and 95% confidence interval was used to find the upper and lower range of the reference shear stress and the hiding function exponent. The hiding function, which increases the mobility of large grain sizes that have a greater surface area exposed to the flow and reduces the mobility of smaller grain sizes that tend to be hidden amongst larger clasts, has the ability to significantly alter the outcome of the sediment transport model. We use the upper and lower limit of the hiding function exponent to assess uncertainty in computations that rely on the Wilcock and Crowe (2003) sediment transport equation.

3.5 Predicting the mobility of bed and bar sediments at bankfull stage

As the calibrated Wilcock and Crowe (2003) sediment transport model determines transport rate for various grain sizes, it can be used to evaluate the mobility of sediments at different reaches in the White Clay Creek watershed. By applying the sediment transport model to the bed and bar grain size distribution at each study site, the largest grain size predicted to be mobile at bankfull conditions is determined based on the dimensionless transport parameter W_{*i}. For these computations, the bankfull depth and reach-averaged bed slope were used to determine shear stresses on both the bar and the streambed. We did not assess differences in shear stress associated with complex bar topography at each site. Grain sizes are no longer considered mobile when $W_{*i} < 0.002$ (Parker et al., 1982). These methods are used to test two of our preliminary hypotheses: 1) that a significant fraction of the bed is immobile at bankfull stage, and 2) that sediments comprising the bar represent stored alluvium that is mobile at bankfull stage.

3.6 Model computations to assess sensitivity to changes in bed material supply

A numerical model was developed to predict changes in bed elevation and grain size over time. The initial conditions—bankfull width, depth, and slope, as well as the grain size distribution of the bed and bar material—are based on surveys and pebble counts conducted at the study sites around the White Clay Creek watershed. While 12 sites are used to characterize the watershed, 8 were selected for use in the numerical model. Four sites were not utilized due to absence of a suitable gravel bar (Sites 2, 9, 10, 11).

The model represents study sites of the White Clay Creek with an idealized geometry. All reaches have a rectangular cross-section. Because only a few grain diameters of aggradation are needed to convert the White Clay Creek to an alluvial channel, changes in slope with time are not computed, so the model domain consists of a short 100 m reach. The models bed is characterized by a mixed or active layer that describes the thickness of bed material accessible to the flow (Parker, 1991, 2008). The thickness of this layer was approximated as $2D_{90}$ and remained constant throughout the simulation. The active layer thickness was based on the D_{90} of the bar, since the bar sediment is fully mobile at bankfull stage.

Changes in grain size distribution with time within the 100 m model domain are computed using equation (2) (Parker, 1991, 2008):

$$(1-\lambda_p)\left[L_a\frac{\partial F_{bi}}{\partial t}+(F_{bi}-F_{li})\frac{\partial L_a}{\partial x}\right]=-\frac{\partial q_{bi}}{\partial x} \tag{2}$$

where λ_p is the porosity of the bed (set equal to 0.3), L_a is the thickness of the active layer, F_{bi} is the fraction of grain size i on the bed, F_{li} is the fraction of grain size i at the interface between the active layer and the subsurface, q_{bi} is the volumetric bed material transport rate per unit width, t is time, and x is the downstream spatial coordinate. In solving equation (2), differential terms are represented by finite differences. For example, the term on the right is approximated as $(q_{bi\ out}q_{bi\ in})/dx$, where $q_{bi\ in}$ is the specified supply of grain size i from upstream, $q_{bi\ out}$ is the transport out of the study

reach computed using the calibrated Wilcock and Crowe (2003) transport equation, and dx is 100 m. The interface grain size fraction, F_{li}, is based on a formulation by Hoey and Ferguson (1994). During erosion, subsurface material is incorporated into the active layer so F_{li} is equivalent to the fraction of grain size i in the subsurface. Alternately, during aggradation, F_{li} is a weighted mixture of sediments currently present in the active layer and bedload, such that $F_{li} = aF_{bi} + (1-a)p_i$, where p_i is the fraction of grain size i in the bedload and a is an exchange parameter (set equal to 0.7).

Once fractional transport rates have been computed by solving equation (2), they are summed to determine the total bed material flux, $q_{b\ Total}$. Changes in bed elevation, z_b, over time are then determined by solving equation (3) (Parker, 1991, 2008):

$$\frac{\partial z_b}{\partial t} = -\frac{1}{(1-\lambda_p)}\frac{\partial q_{b\ Total}}{\partial x} \tag{3}$$

Numerical experiments were designed to test two key hypotheses of our conceptual model: (1) the study reaches are undersupplied relative to the capacity of the White Clay Creek to transport bed material, and (2) the grain size distribution of the bed material reflects the grain sizes supplied from upstream in addition to grain sizes supplied locally. To test these hypotheses, computations proceed in the following manner. First, the existing sediment transport capacity of each site is defined by computing transport rates determined using the calibrated Wilcock and Crowe (2003) equation and the observed bed material grain size distribution. This quantity is denoted $Q_{bT\ bed}$. Then, the supply from upstream consisting of grain sizes observed on the bar is then set for each model run, and the bed and grain size distribution evolve through time, while the width and slope remain unchanged. Simulations were run for 20,000 days of bankfull flow or until the bed material grain size distribution ceased to change with time (see (Bodek, 2020), for additional details). We use the term equilibrium to refer to conditions at the end of the simulation regardless of the criteria used to stop the run. The bed material transport rate in the simulated reach at the end of the simulation is termed $Q_{bT\ eq}$.

Conditions at the end of each run determine if the imposed bed material supply results in the establishment of an alluvial or a non-alluvial channel. An alluvial channel results when (1) the bed aggrades to cover the non-fluvial material on the bed of the reach or (2) the equilibrium bed grain size distribution represents that of the throughput load entering the reach (Table 3). The first condition occurs when the equilibrium bed aggrades to an elevation that reaches or surpasses the thickness of the active layer, which is based on the D_{90} of the bar material ($L_a = 2D_{90\ bar} = 0.2m$). The second condition occurs when the mean grain size, D_m, of the equilibrium bed matches the mean grain size of the throughput load supplied from upstream ($D_{m\ eq} = D_{m\ bar}$). By varying the supply of bed material, and hence the ratio $Q_{bT\ eq}/Q_{bT\ bed}$, these numerical experiments determine how much additional sediment supply would be needed to transform the White Clay Creek into an alluvial channel whose bed material solely reflects sediment supplied by fluvial transport.

4 Results

4.1 Longitudinal profile

The longitudinal profile of the White Clay Creek reveals a knickpoint where the East Branch flows through a steep-walled, bedrock gorge slightly north of Landenberg, PA (Figure 1b). The knickpoint separates the longitudinal profile into two concave-upwards segments. The projection of the upstream segment near Newark, DE is at the same elevation as the Old College Formation, suggesting that these alluvial fan sediments were deposited by an ancestral White Clay Creek. The downstream concave upwards segment of the profile is lower than the Old College Formation (Figure 1b, c), indicating that the

Table 3. Possible Outcomes of the Numerical Model and their Interpretation

Variable	Outcome	Description
Bed elevation, z_b	$\Delta z_b = L_a$, $\Delta z_b > L_a$	Alluvial conditions reached; bed has aggraded to cover non-alluvial material
	$0 < \Delta z_b < L_a$	Alluvial-colluvial-bedrock channel persists with some aggradation
	$\Delta z_b < 0$	Alluvial-colluvial-bedrock channel persists with some erosion of bed material
Mean grain size, D_m	$D_{m\ eq} = D_{m\ bar}$, $D_{m\ eq} < D_{m\ bar}$	Alluvial conditions reached; bed GSD has fined and is representative of the throughput load entering the reach
	$D_{m\ eq} > D_{m\ bar}$	Alluvial-colluvial-bedrock channel persists with some fining of the bed material

knickpoint has migrated upstream since the deposition of the Old College Formation, incised approximately 50 m into the underlying crystalline bedrock, and is likely providing a supply of boulder and cobble-size clasts to the channel of the White Clay Creek.

4.2 Reach-scale geomorphic characterization

Geomorphic mapping reveals typical landforms developed at the sites (Figure 3a). The channel at Site 4 is gently curving, with well-developed pools, riffles, and runs. Boulders are scattered across the bed, some exceeding 1 m in diameter. The channel occasionally encounters bedrock and the colluvium of the valley margin in one of its banks; a short section is confined by a 19^{th} century railroad grade. Four bars have developed across the channel from eroding banks at the outsides of bends; new laterally accreted floodplains have formed adjacent to two of these bars. Several side channels are accessed during high flows.

Figure 3b illustrates typical landforms in cross-section. The eroding bank on the right side of the cross-section features cohesive sand and mud that extends all the way to the streambed, indicating that gravel bed material does not influence bank stability. Deposits of the eroding bank feature a well-developed buried A-horizon, a paleosol generally interpreted to represent the boundary between older deposits pre-dating European colonization and younger deposits post-dating European colonization (Jacobson & Coleman, 1986; Walter & Merritts, 2008). Sandy laterally accreted floodplain deposits are exposed on the left side of the cross-section, adjacent to sandy bar deposits of the streambed; these are typical of mid-Atlantic streams (Jacobson & Coleman, 1986; Merritts et al., 2013; Walter & Merritts, 2008).

The 12 study sites have bankfull widths of 9.9–36.03 m, bankfull depths of 0.77–2.75 m, and slopes from 0.0008–0.0067 (Table 4). Bank retreat rates vary from 2.6–32.1 cm/yr. Median bed material grain sizes range from 18.7–90 cm, with half of the sites displaying median bed grain sizes in the pebble-size range and half in the cobble-size range. The sand fraction of the bed material ranges from 0.09–0.28. The median grain sizes of bars are all in the pebble size range, varying from 15.2–34.5 cm. Bars generally store less sand that the streambed, with sand fractions ranging from 0.078–0.157. Bar sediments are notably finer than sediments of the streambed (Figure 4).

Bankfull Shields stresses based on the median grain size of the bed material range from 0.02 to 0.15 (Table 4). Dividing these values by the threshold Shields stress of 0.056 estimated from our tracer data (presented below) yields ratios 0.41–2.63. These data fall

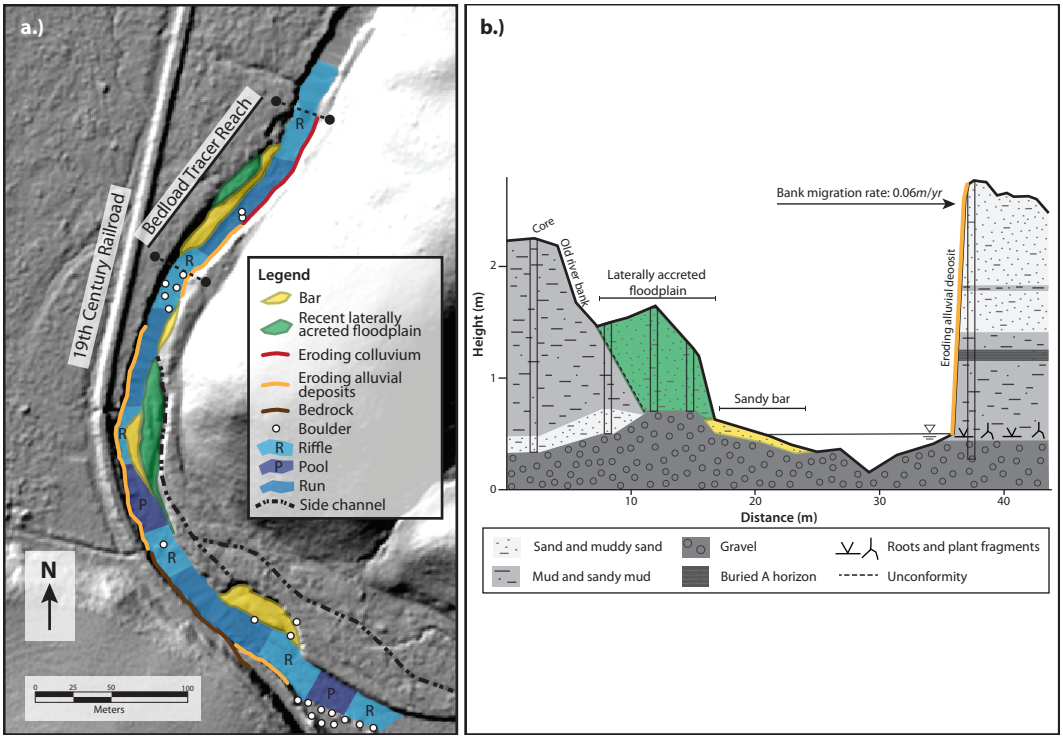

Figure 3. Representative geomorphic map and cross-section. (a) Geomorphic map of Site 4, which encompasses the bedload tracer study reach; (b) Cross-section at Site 1 showing typical stratigraphic relationships between landforms and a fully cohesive eroding bank.

Table 4. Reach-scale Morphology and Sediment Transport Processes at the Study Sites

Site no.	Bankfull width	Bankfull depth	Slope	Median grain size		Fraction sand		τ_{*bf}	$\frac{\tau_{*bf}}{\tau_{*rm}}$	Lateral bank retreat rate
				$D_{50\ bed}$[a]	$D_{50\ bar}$[a]	$F_{s\ bed}$	$F_{s\ bar}$			
	[m]	[m]	[–]	[mm]	[mm]	[–]	[–]	[–]	[–]	[cm/yr]
1	22.47	2.75	0.0037	67.6	30.1	0.19	0.11	0.091	1.629	6.2
2	36.03	1.92	0.0008	40.2	NA[b]	0.13	0.55	0.023	0.414	32.1
3	15.19	1.19	0.0039	55.5	34.0	0.26	0.11	0.051	0.905	20.1
4	27.55	1.87	0.0055	57.9	23.9	0.13	0.08	0.108	1.922	5.8
5	21.06	2.16	0.0029	83.2	33.7	0.07	0.12	0.046	0.815	13.0
6	26.49	1.78	0.0045	79.5	27.7	0.11	0.09	0.061	1.090	4.9
8	14.71	1.70	0.0031	46.5	15.2	0.18	0.16	0.069	1.227	19.0
9	14.57	1.80	0.0024	28.4	ND[c]	0.28	ND	0.092	1.646	9.8
10	9.90	0.77	0.0059	18.7	ND	0.19	ND	0.147	2.629	12.4
11	12.75	1.15	0.0056	34.2	ND	0.14	ND	0.114	2.038	2.6
12	30.43	1.76	0.0046	81.4	30.9	0.10	0.10	0.060	1.076	9.1
14	22.45	1.90	0.0067	90.0	34.5	0.07	0.09	0.086	1.531	12.1

[a]Sand-sized sediment ($< \ 2mm$) was excluded from the grain size distribution when determining median grain size. This is because sand-sized sediment is expected to be transported in suspension during bankfull flows. [b]NA—not applicable. [c]ND—no data: some study sites lacked a well-developed gravel bar.

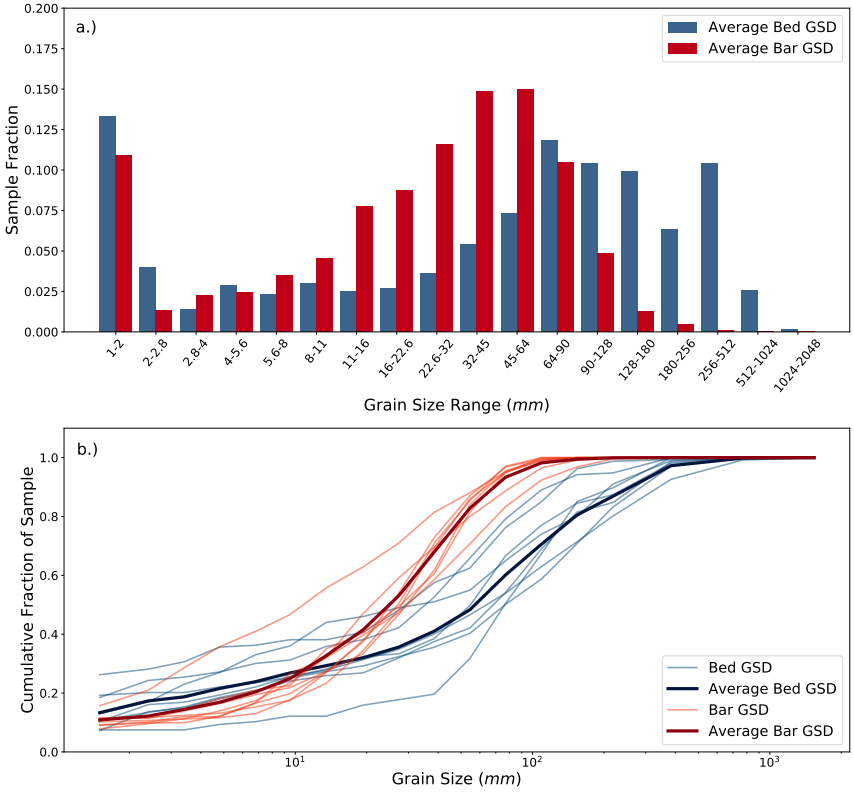

Figure 4. Grain size distributions for sediment in the White Clay Creek watershed: (a) average grain size distribution for bed and bar material, (b) cumulative grain size distribution for bed and bar material at 8 sites. Average bed and bar cumulative grain size distributions are also displayed. Average grain size distributions are based on pebble counts at Sites 1, 3, 4, 5, 6, 8, 12, and 14.

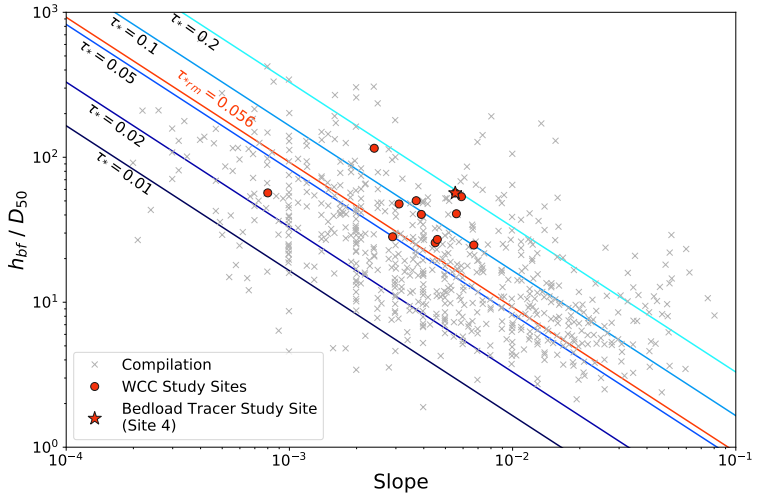

Figure 5. Bankfull relative submergence and slope for the White Clay Creek study sites and a compilation of data from alluvial near-threshold gravel-bed rivers from Phillips and Jerolmack (2019). Diagonal lines indicate values of constant Shields stress. The threshold Shields stress for incipient motion determined from bedload tracer studies at Site 4 of the White Clay Creek is indicated in red.

within the range expected for alluvial near-threshold gravel-bed rivers (Figure 5), an interpretation that would require a fully mobile bed at bankfull stage and implies an adjustment of channel morphology to the supply of bed material.

4.3 Bedload tracer particles

Four flows occurred during the active monitoring of tracer particles with stages that equaled or exceeded 1.86 m. The stage of 1.86 m is 2/3 of the action stage (referred to as bankfull hereafter) of 2.74 m defined by the USGS at the Strickersville gaging station. Three flows reached 2/3 of the bankfull stage (documented by surveys on 2 July 2019, 25 July 2019, and 5 November 2019), while the fourth event reached 92% of the bankfull stage (documented by a survey on 28 January 2020). Additional details are provided by Bodek (2020).

Based on cumulative results from the nine surveys, smaller grains tend to be more mobile than larger grains. Tagged clasts in the 11–45 mm size range were observed to have moved the most during the study period (Figure 6). Mobility decreases as clasts become larger, with limited motion above 180 mm and no motion observed above 512 mm.

Data from events on 27 October 2019 and 25 January 2020 are used to calibrate the Wilcock and Crowe (2003) bedload transport equation. During the first event, the stage at the Strickersville gage height reached 1.86 m. The subsequent survey of bedload tracer particle locations indicated that 84.6% of the relocated tagged clasts were immobile (with a 93% recovery rate). Only smaller clasts (<8 cm) were transported by this event. During the second event, the Strickersville gage reached 2.52 m (92% of bankfull stage). This event mobilized 59.5% of the located tracers (with a 66% recovery rate). The largest mobile clast was 45 cm.

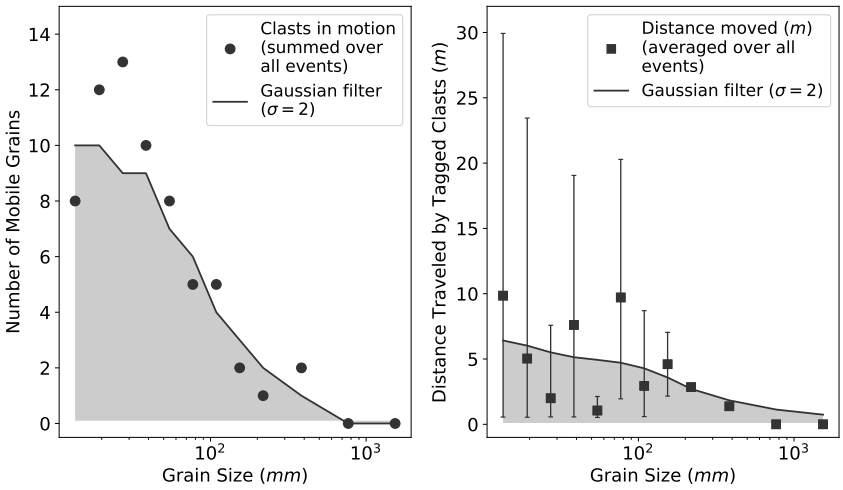

Figure 6. Mobility of each grain size category based on cumulative results from nine surveys: (a) number of clasts in motion summed over all nine events; (b) average distance traveled by tagged clasts per event. The error bars indicate individual events with the shortest and longest distance traveled. Both the number of tracer particles in motion and average distance traveled by tagged particles increases for smaller clasts.

On 4 August 2020, 7 months after active monitoring of the tracer particles had ended, rainfall from Tropical Storm Isaias resulted in a peak stage of 3.99 m at the White Clay Creek gaging station near Strickersville. This event, estimated as a 50-yr flood (Gerald Kauffman, personal communication) at the White Clay Creek near Newark (USGS gaging station #01479000), was followed 3 days later by a peak stage of 3.47 m at the Strickersville gage as a result of unusually intense thunderstorms.

Tracer particles were resurveyed on 14 August 2020. Because multiple large events had occurred between surveys (including a near-bankfull event on 13 April 2020), only qualitative results could be obtained. Only 13 of the 54 tagged particles were found; these included nine boulders (all tagged boulders were found), three cobbles, and one pebble. Of these, four boulders with diameters from 340 mm to 800 mm moved a median distance of 1.5 m; one 450 mm boulder moved 39.4 m. The remaining boulders, with diameters from 420–1440 mm, did not move. One cobble moved 28.9 m, while the other two cobbles were immobile. The 60 mm diameter pebble did not move. These data demonstrate that rare, extreme events will move some boulders short distances, while others remain immobile during even these exceptional discharges.

4.4 Bedload transport model calibration

To calibrate the Wilcock and Crowe (2003) transport equation, it is necessary to determine the reference shear stress of each grain size category. By plotting the reference shear stress of each grain size against normalized grain size (Figure 7), the reference shear stress for the mean grain size (τ_{rm}) and hiding function exponent (b) can be determined through linear regression:

$$\tau_{ri} = 23.95 \left(\frac{D_i}{D_m} \right)^{0.23} \tag{4}$$

where the coefficient indicates the reference shear stress of the mean grain size ($\tau_{rm} = 23.95$ kg/ms^2) and the exponent ($a = 0.23$) is related to the hiding function exponent

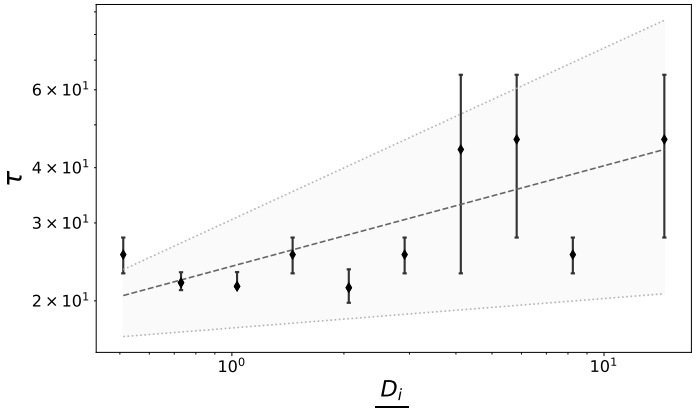

Figure 7. Reference shear stress is related to dimensionless grain size by a power function, where grain size is normalized by the mean grain size. Error bars indicate the range of reference shear stresses possible for each grain size based on bedload tracer data. The light gray lines bounding the trend line indicate a 5% and 95% confidence interval.

(b) as $b = a-1$. Including the 95% confidence interval yields $\tau_{rm} = 23.95 \pm 6.58$ kg/ms^2 and $a = 0.23 \pm 0.16$.

The dimensionless reference shear stress for the mean grain size, τ_{*rm}, is 0.056$\pm$ 0.015. The hiding function exponent, b, is 0.77$\pm$0.16. This yields the relationship between reference Shield's stress and normalized grain size:

$$\tau_{*ri} = 0.056 \left(\frac{D_i}{D_m} \right)^{-0.77} \tag{5}$$

4.5 Bed and bar sediment mobility at bankfull stage

The calibrated Wilcock and Crowe (2003) equation indicates that the largest clast on the bed at Site 4 that is expected to be mobile at bankfull stage is 187.0 mm, while the largest mobile clast on the bar is 198.4 mm. The largest mobile grain size differs for the Site 4 bed and bar material due to the hiding function. Thus, 85.7% of the bed material should be mobile at bankfull stage, while almost 100% of the bar material should be mobile under the same conditions (Table 5). Within the White Clay Creek Watershed, 92–100% of the bar material is expected to be mobile at bankfull stage, while only 27–92% of bed material is mobile.

Bodek (2020) supplements the estimates of bed mobility presented here based on the Wilcock and Crowe (2003) equation with additional bed mobility estimates based on the Shields diagram and threshold mobility values reported by Buffington and Montgomery (1997). While these analyses are not included here, the two methods generally provide similar results.

4.6 Excess capacity of the White Clay Creek to transport bed material

Numerical model estimates of the ratio of $Q_{bT\ eq}/Q_{bT\ bed}$ needed to entirely cover the active layer range from 1.23 to 1.90 across the eight modeled study sites, suggesting that a roughly 20–90% or greater increase in bed material supply would be needed

Table 5. Competence of WCC Study Sites Based on the Calibrated Wilcock and Crowe (2003) Sediment Transport Model

Site no.	Median grain size		Largest mobile grain size		Range of Largest Mobile Grain Size		Percent mobile		Range of mobile material	
	$D_{m\ bed}$[a] [mm]	$D_{m\ bar}$[a] [mm]	$D_{mobile\ bed}$ [mm]	$D_{mobile\ bar}$ [mm]	$D_{mobile\ bed}$ [mm]	$D_{mobile\ bar}$ [mm]	Bed [%]	Bar [%]	Bed [%]	Bar [%]
1	34.5	22.2	156.2	151.1	132.6–255.5	135.1–153.2	84.6	100.0	80.9-89.8	100.0
2	26.8	2.3	15.6	26.6	13.0–17.9	19.3–27.2	27.1	100.0	24.4–29.6	100.0
3	18.4	22.7	73.0	69.7	54.4–101.7	54.2–88.7	73.8	91.8	62.5–83.0	83.7–97.0
4	26.4	21.8	187.0	198.4	138.1–338.6	140.0–352.9	85.7	99.7	77.9–96.8	98.3–100.0
5	65.5	21.3	73.6	103.1	73.4–73.9	76.2–148.2	47.6	98.2	47.4–47.9	94.5–99.9
6	44.9	21.9	107.8	142.2	101.0–141.5	104.4–201.6	68.4	99.9	65.3–78.0	99.1–100
8	22.2	11.3	76.5	100.6	68.0–106.9	71.2–162.7	78.9	98.0	73.8–88.4	93.4–100
9	11.1	ND[b]	75.0	ND	53.8–123.4	ND	91.0	ND	84.4–96.2	ND
10	14.3	ND	74.7	ND	54.3–108.5	ND	92.0	ND	85.0–96.6	ND
11	24.0	ND	103.2	ND	76.6–145.7	ND	92.0	ND	83.8–97.2	ND
12	47.0	23.7	107.9	136.7	101.6–140.3	104.7–151.1	62.6	100.0	60.9–68.8	99.3–100
14	50.7	26.0	202.1	246.0	152.6–316.5	157.4–433.0	80.1	99.6	70.4–91.5	97.0–100
Avg[c]	30.2	16.2	106.7	134.5	90.8–147.8	96.5–214.1	77.1	99.1	72.5–84.7	96.7–99.9
Avg[d]	37.9	20.7	122.3	147.1	103.9–153.7	106.0–240.7	73.5	99.3	68.9–80.4	97.8–99.9

Note. The largest mobile grain size is determined using the Wilcock and Crowe (2003) sediment transport equation that has been calibrated to conditions at the bedload tracer study site. The range of largest mobile grain sizes is based on the range of hiding function exponents ($b = 0.93$ and $b = 0.61$) determined by the 5% and 95% confidence interval of the bedload tracer mobility data.
[a]Sand-sized sediment ($< 2mm$) was included in the grain size distribution when determining mean size. [b]ND—no data; some study sites lacked a well-developed gravel bar. [c]Average for all 12 study sites. [d]Average for 8 study sites with well developed gravel bars present (Site 1, 2, 3, 4, 5, 6, 8, 12, 14)

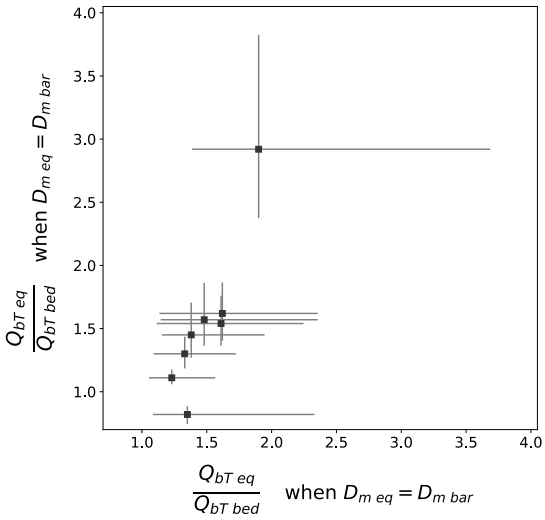

Figure 8. The ratio of sediment fluxes ($Q_{bT\ eq}/Q_{bT\ bed}$) at which the modeled reaches develop alluvial characteristics. The x-axis depicts the ratio of fluxes when the equilibrium bed elevation of a modeled reach has aggraded to cover the active layer. The y-axis indicates the ratio of fluxes when the mean grain size of the equilibrium bed matches the mean grain size of the bar material, which is representative of the throughput load. The error bars indicate the range of outcomes based on the 95% confidence interval of the hiding function exponent.

to transform the White Clay Creek into an alluvial channel (Figure 8). The ratio of sediment fluxes that caused the mean grain size of the equilibrium bed to match that of the bar ranges from 1.3 to 2.92 across seven of the eight study sites. The one study site with contradicting results is Site 3, where the mean grain size of the bed material is finer than the bar material. With the exception of Site 3, an 11–200% increase in fluvially transported material would be needed to equalize the grain size distributions of the bed and bar sediments.

The two criteria used to determine if a modeled reach has developed alluvial characteristics generally agree across the different study sites (Figure 8). Thus, an insensitive site that requires a significant increase in the flux of throughput load to fine the bed also requires a similarly significant increase for the bed to aggrade. This trend does not apply to Site 3, where the mean grain size of the bed is finer than the mean grain size of the bar.

5 Discussion

While bankfull Shields stresses of the White Clay Creek fall within the ranges typically observed for alluvial near-threshold gravel-bed rivers with stable banks, other data indicate that this interpretation is untenable. The long profile morphology shows clear evidence of long-term bedrock incision, and geomorphic mapping indicates that the influence of bedrock and colluvium on the White Clay Creek is ongoing. Tracer studies and computations with the calibrated Wilcock and Crowe (2003) bedload transport equation indicate that a substantial portion (8–73%) of the bed is immobile at bankfull stage, whereas in alluvial near-threshold gravel-bed rivers, the bed is expected to be fully mobile. Numerical simulations suggest that the channel is undersupplied by sediment, such that significant increases in bed material supply could be readily accommodated by chang-

ing grain size alone, rather than by changes in channel geometry. Banks are cohesive throughout their vertical extent, so gravel mobility is unrelated to bank stability. Thus, the morphology of the White Clay Creek is neither sensitive to, nor adjusted to the supply of bed material. It cannot be considered an alluvial near-threshold gravel-bed river despite Shields stresses based on D_{50} that are slightly in excess of the threshold of motion.

While the White Clay Creek is clearly not an alluvial near-threshold gravel-bed river, it is still reasonable to consider the bed of the White Clay Creek to be near-threshold. This interpretation is supported by the population of grains that are immobile at bankfull stage, indicating that some grain size fractions must be close to the threshold of motion. However, the median grain size does not well-represent the bed of the White Clay Creek because the bed material consists of two separate populations, a finer population supplied from upstream and a coarser population supplied locally by erosion of bedrock and colluvium. Viewed in this way, it appears that the White Clay Creek behaves more like a threshold colluvial-bedrock channel than an alluvial channel, with a bed anchored by immobile coarse sediment and a partial covering of mobile throughput alluvium.

These ideas are illustrated in Figure 9, which presents a provisional classification of threshold rivers by grain size and the percentage of the bed that is mobile at bankfull stage. The three categories of threshold channels defined previously in the literature appear as distinct end-members. Alluvial channels with fully mobile sand and gravel beds occupy narrow regions at the top of the diagram with 100% bed mobility, while colluvial/bedrock threshold channels occupy another distinct narrow band at the bottom of the diagram, where bed mobility is 0. Between these end-members is a large domain that represents a continuum of channels with partially immobile beds that we term threshold alluvial-colluvial-bedrock channels. Data from the White Clay Creek mostly plot at the upper end of this continuum, implying that even a small fraction of large, immobile grains (and relatively infrequent exposures of bedrock) can induce non-alluvial streambed behavior, a hypothesis that is supported by recent flume studies (MacKenzie & Eaton, 2017; MacKenzie et al., 2018). Observations from many other rivers are needed, however, to better define the categories and behavior of threshold channels in Figure 9.

5.1 Width adjustment and cohesive bank erosion threshold

Bank erosion thresholds play an important role in explanations of the reach-scale morphology of alluvial rivers. Cohesive bank erosion thresholds have been cited as a control of the morphology of sand-bed channels (Dunne & Jerolmack, 2018), and they also feature prominently in some analytical models of hydraulic geometry (Huang & Nanson, 1998; Millar & Quick, 1993, 1998). Near-threshold alluvial gravel-bed rivers adjust their morphology to achieve erosion thresholds for gravel at the bank toe (Parker, 1978).

Eroding banks occur frequently along the White Clay Creek (Table 1), and while erosion may occur in a variety of settings (Donovan et al., 2015; Merritts et al., 2013), it is often focused by curvature at the outsides of bends (Allmendinger et al., 2005; Pizzuto & Meckelnburg, 1989). This suggests that bank erosion is typically accompanied by lateral channel migration, with erosion on the outsides of banks balanced by the creation of new floodplains on the insides of banks (Figure 3). Under these conditions, the appropriate criterion for maintaining a stable width is a balance between rates of lateral accretion and bank migration (Allmendinger et al., 2005). This does not appear to obviously involve bank erosion thresholds, and it requires bank erosion to occur, which seems incompatible with the concept of stable banks adjusted to the threshold of bank erosion.

It has been noted, however, that even laterally active channels, if appropriately averaged, can have a morphology that is consistent with threshold channel behavior (Reitz et al., 2014). Thus, it is conceivable that even though the White Clay Creeks banks are

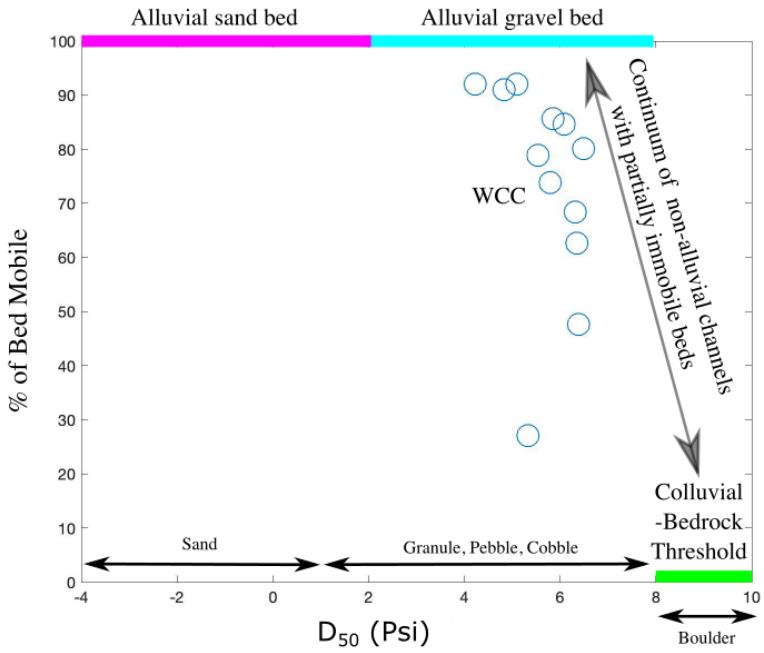

Figure 9. Classification of threshold river channels based on median grain diameter and percentage of mobile bed material. Data from the White Clay Creek are plotted for reference. Grain sizes are plotted using the Psi (Ψ) scale (Parker, 2008), defined by $ln(D_{50})/ln(2)$, with D_{50} in mm.

eroding and its channel is laterally migrating, cohesive bank erosion thresholds may at least partly explain its channel morphology.

Allmendinger et al. (2005) present a simple analysis to explain the width of laterally migrating channels that can be adapted to illustrate a possible (though speculative) role of cohesive bank erosion thresholds in scaling channel width. Rates of lateral accretion, L_A, on inner banks are set equal to rates of outer bank erosion B_E, which in turn are proportional to the near-bank velocity U_b and a cohesive erosion threshold velocity, U_c:

$$L_A = B_E = E(U_b - U_c) \tag{6}$$

where E is a dimensionless erodibility coefficient (Pizzuto & Meckelnburg, 1989). Following Allmendinger et al. (2005), U_b is scaled by the reach-averaged velocity U and a dimensionless parameter u_b that includes the effects of friction and channel curvature (Johannesson & Parker, 1989). U is replaced by Q/WD, where W is the width. Solving the resulting expression for width (and rearranging) yields an expression for the stable width:

$$W = \frac{Qu_b}{EU_c}\left(\frac{1}{\frac{L_A}{EU_c}+1}\right) \tag{7}$$

Equation (7) may be interpreted in the following way. If banks are stable and the rate of lateral accretion is 0, then the expression on the right in parentheses is 1, and the ratio Qu_b/EU_c represents the width of a channel with threshold banks. If the channel is migrating slowly (as is typical for the White Clay Creek), then the rate of lateral accretion will be low, and the ratio L_A/EU_c is will be $\ll 1$, because L_A is scaled by the difference U_bU_c, rather than the velocity itself. Under these conditions, the quantity in parentheses on the right of equation (7) will be only slightly greater than one, allowing for channel width to be only slightly greater than the threshold width and the width itself to scale

with the bank erosion threshold velocity U_c. Equation (7) also provides a mechanism for width to vary with discharge, allowing for downstream hydraulic geometry relationships such as those presented for the nearby Brandywine Creek by Wolman (1955).

This analysis is not intended to be either comprehensive or precise, and it is admittedly simplistic and speculative. The assumption of an equilibrium width, for example, is difficult to justify given the dramatic changes to watersheds of the region outlined below. Equation (7), however, does present a hypothesis to explain how width scaling by cohesive bank erosion thresholds could arise even when channels are laterally active, thereby providing a link between the White Clay Creek and proposed scaling of alluvial sand-bed and gravel-bed channels by cohesive bank erosion thresholds. Further research is clearly warranted, of course, to more fully test these ideas.

5.2 Current and past anthropogenic influences

Humans have had a profound influence on streams and watersheds of the region that predates European colonization (James, 2019) and continues at present. The supply of water and sediment to stream channels has varied in response to changes in land use and land cover, and streams themselves have been directly impacted by a variety of human activities in river corridors over time. These impacts operate over multiple timescales, and many geomorphologists have suggested that past activities still influence streams of the region, even as ongoing processes drive contemporary changes in streams and their morphology (Jacobson & Coleman, 1986; Walter & Merritts, 2008; Wolman, 1967).

While human and natural influences on stream channels and riparian areas are too diverse and complex to explore fully here, one result is important to highlight: the Holocene record of valley-fill deposits that are exposed in the channel margins of the White Clay Creek (illustrated in Figure 3). These deposits create a variety of surfaces representing differing elevations, depositional processes, and periods in the history of the White Clay Creek. For example, in Figure 3b, the thickness of the deposits on the right side of the cross-section is at least partly controlled by depositional processes active during colonial times. These deposits, and the high-elevation landform they create, are slowly being removed by bank erosion, while new, lower elevation deposits are forming on the left side of the cross-section.

The complexity of the topography in Figure 3 presents important concerns regarding the use of the bankfull Shields parameter as a metric for identifying threshold stream channels. In a cross-section such as Figure 3b, it is unclear whether a bankfull stage can be objectively identified, or even if the concept of a channel-forming bankfull stage is meaningful. Rather than relying on a questionable metric, it is better in these circumstances to actually measure rates of sediment transport processes directly, even though such measurements are difficult and time-consuming.

Mill dams constructed after European colonialization represent another ongoing influence on stream channels that has recently been recognized (Merritts et al., 2011, 2013; Walter & Merritts, 2008). These low-head, run-of-river dams are common in the White Clay Creek, and extant or breached mill dams are located within a few kilometers upstream or downstream of 8 of our 12 study sites (Table 1). It is very unlikely that these mill dams influence the hydrologic regime of the White Clay Creek, and Pearson and Pizzuto (2015) demonstrate that gravel bed material may be transported through the impoundments created by extant mill dams on these streams. It is unlikely, therefore, that these historic structures have any significant influence on bed material transport processes at our study sites. Some deposits in channel margins of our study sites may owe their origins to historic mill dams, but documenting the spatial extent of mill dam deposits is outside the scope of this study, and is the focus of ongoing research.

6 Conclusions

Our observations and interpretations suggest that the White Clay Creek is a threshold alluvial-colluvial-bedrock river with a partially mobile bed at bankfull stage. It appears to represent an example of a continuum of gravel-bed, alluvial-colluvial-bedrock rivers, with end-members representing near-threshold alluvial gravel-bed rivers with fully mobile beds at bankfull stage and colluvial-bedrock threshold channels whose perimeter is entirely composed of immobile bed material. Because the bed of the White Clay Creek is composed of two populations of sediment, analyses based on a single grain size such as the bankfull Shields stress scaled by D_{50} are unlikely to be useful, motivating a more thorough analysis of sediment transport processes by that incorporates the mobility of individual grain size fractions.

By expanding our analysis beyond bedload transport processes to include bank stratigraphy and bank erosion processes, other important insights are gained. The White Clay Creek is not only a threshold channel because some of its bed material is near the threshold of motion at bankfull stage, but its width may also be scaled by cohesive bank erosion processes. We argue that even though banks cannot be precisely adjusted to bank erosion thresholds (because erosion is pervasive and channels are actively migrating), thresholds of bank erodibility may nonetheless provide useful approximate scaling relationships for interpreting channel morphology. Analysis of bank stratigraphy also reveals the morphologic record of recent watershed disturbances that continue to influence channel morphology, and that complicate interpretation of channel processes based on simple indices such as the bankfull Shields stress.

While the present study focuses on a single watershed, our analyses may have identified a common, though underappreciated, category of stream channels. The supply of coarse sediment from local sources is not an unusual occurrence, and channel perimeters composed of cohesive sediments related to anthropogenic watershed disturbances have been widely reported (Happ et al., 1940; Trimble, 1981; Walter & Merritts, 2008; Wilkinson & McElroy, 2007). Fluvial geomorphologists will need to look beyond simple sediment transport metrics to fully understand and adequately classify these stream channels.

Acknowledgments

Financial support was provided by Delaware Watershed Research Fund Award #DWRF-16-109. Doug Jerolmack and Colin Phillips loaned instrumentation needed for tracking bedload tracer particles. Useful suggestions were offered by Melinda Daniels, Doug Jerolmack, and John Pitlick. Supporting data can be found in Bodek (2020) and McCarthy (2018), which are available through the ProQuest Dissertations & Theses database.

Attribution: SB performed the bedload transport monitoring and analysis, KMM and RA surveyed the 12 study sites, KMM quantified bank erosion rates, and JEP supervised all aspects of the study.

References

Allmendinger, N. E., Pizzuto, J. E., Potter Jr, N., Johnson, T. E., & Hession, W. C. (2005). The influence of riparian vegetation on stream width, eastern Pennsylvania, USA. *Geological Society of America Bulletin*, *117*(1–2), 229–243. doi: 10.1130/B25447.1

Andrews, E. D. (1984). Bed-material entrainment and hydraulic geometry of gravel-bed rivers in Colorado. *Geological Society of America Bulletin*, *95*(3), 371–378. doi: 10.1130/0016-7606(1984)95⟨371:BEAHGO⟩2.0.CO;2

Andrews, E. D., & Parker, G. (1987). Formation of a coarse surface layer as the

response to gravel mobility. In C. R. Thorne, J. C. Bathurst, & R. D. Hey (Eds.), *Sediment transport in gravel-bed rivers* (pp. 239–300). New York, NY: Wiley.

Bodek, S. (2020). *Is the White Clay Creek a threshold channel? Evaluating bed-mobility of a gravel-bed river, Pennsylvania, U.S.A.* (Unpublished master's thesis). University of Delaware, Newark, DE.

Buffington, J. M., & Montgomery, D. R. (1997). A systematic analysis of eight decades of incipient motion studies, with special reference to gravel-bedded rivers. *Water Resources Research*, *33*(8), 1993–2029. doi: 10.1029/96WR03190

Church, M. (2006). Bed material transport and the morphology of alluvial river channels. *Annual Review of Earth and Planetary Science*, *34*, 325–354. doi: 10.1146/annurev.earth.33.092203.122721

Dade, W. B., & Friend, P. F. (1998). Grain-size, sediment-transport regime, and channel slope in alluvial rivers. *Journal of Geology*, *106*(6), 661–676. doi: 10.1086/516052

Diplas, P., & Vigilar, G. (1992). Hydraulic geometry of threshold channels. *Journal of Hydraulic Engineering*, *118*(4), 597–614. doi: 10.1061/(ASCE)0733-9429(1992)118:4(597)

Donovan, M., Miller, A., Baker, M., & Gellis, A. (2015). Sediment contributions from floodplains and legacy sediments to Piedmont streams of Baltimore County, Maryland. *Geomorphology*, *235*, 88–105. doi: 10.1016/j.geomorph.2015.01.025

Dunne, K. B., & Jerolmack, D. J. (2018). Evidence of, and a proposed explanation for, bimodal transport states in alluvial rivers. *Earth Surface Dynamics*, *6*(3). doi: 10.5194/esurf-6-583-2018

Fischer, J. M., Riva-Murray, K., Hickman, R. E., Chichester, D. C., Brightbill, R. A., Romanok, K., & Bilger, M. D. (2004). *Water quality in the Delaware River Basin, Pennsylvania, New Jersey, New york, and Delaware, 1999-2001* (Vol. Circular 1227). Reston, VA: US Geological Survey.

Glover, R. E., & Florey, Q. L. (1951). *Stable channel profiles* (No. Hyd-325). Washington, DC: U.S. Bureau of Reclamation, Design and Construction Division.

Hack, J. T. (1982). *Physiographic divisions and differential uplift in the Piedmont and Blue Ridge* (No. 1265). Reston, VA: U.S. Geological Survey.

Happ, S. C., Dobson, G. C., & Rittenhouse, G. (1940). *Some principles of accelerated stream and valley sedimentation* (No. 695). Washington, DC: U.S. Department of Agriculture.

Hoey, T. B., & Ferguson, R. (1994). Numerical simulation of downstream fining by selective transport in gravel bed rivers: Model development and illustration. *Water Resources Research*, *30*(7), 2251–2260. doi: 10.1029/94WR00556

Huang, H. Q., & Nanson, G. C. (1998). The influence of bank strength on channel geometry: an integrated analysis of some observations. *Earth Surface Processes and Landforms*, *23*(10), 865–876. doi: 10.1002/(SICI)1096-9837(199810)23:10⟨865::AID-ESP903⟩3.0.CO;2-3

Jacobson, R. B., & Coleman, D. J. (1986). Stratigraphy and recent evolution of Maryland Piedmont flood plains. *American Journal of Science*, *286*(8), 617–637. doi: 10.2475/ajs.286.8.617

James, L. A. (2019). Impacts of pre-vs. postcolonial land use on floodplain sedimentation in temperate North America. *Geomorphology*, *331*, 59–77. doi: 10.1016/j.geomorph.2018.09.025

Johannesson, H., & Parker, G. (1989). Linear theory of river meanders. In S. Ikeda & G. Parker (Eds.), *River meandering* (Vol. 12, p. 181-214). Washington DC: Americal Geophysical Union. doi: 10.1029/WM012p0181

Johnson, J. P. L., Whipple, K. X., Sklar, L. S., & Hanks, T. C. (2009). Transport slopes, sediment cover, and bedrock channel incision in the Henry Moun-

763 tains, Utah. *Journal of Geophysical Research: Earth Surface*, *114*. doi:
764 10.1029/2007JF000862
765 Kauffman, G. J., & Belden, A. C. (2010). Water quality trends (1970 to 2005) along
766 Delaware streams in the Delaware and Chesapeake Bay watersheds, USA. *Wa-*
767 *ter, air, and soil pollution*, *208*(1-4), 345–375. doi: 10.1007/s11270-009-0172
768 -z
769 Kuhnle, R. A. (1993). Incipient motion of sand-gravel sediment mixtures. *Jour-*
770 *nal of Hydraulic Engineering*, *119*(12), 1400–1415. doi: 10.1061/(ASCE)0733
771 -9429(1993)119:12(1400)
772 Li, R.-M., Stevens, M. A., & Simons, D. B. (1976). Morphology of cobble streams
773 in small watersheds. *Journal of the Hydraulics Division, ASCE*, *102*(8), 1101–
774 1117.
775 MacKenzie, L. G., & Eaton, B. C. (2017). Large grains matter: contrasting bed
776 stability and morphodynamics during two nearly identical experiments. *Earth*
777 *Surface Processes and Landforms*, *42*(8), 1287–1295. doi: 10.1002/esp.4122
778 MacKenzie, L. G., Eaton, B. C., & Church, M. (2018). Breaking from the aver-
779 age: Why large grains matter in gravel-bed streams. *Earth Surface Processes*
780 *and Landforms*, *43*(15), 3190–3196. doi: 10.1002/esp.4465
781 Mackin, J. H. (1948). Concept of the graded river. *Geological Society of America*
782 *Bulletin*, *59*(5), 463–512.
783 McCarthy, K. M. (2018). *Riverbank erosion rates in the White Clay Creek Water-*
784 *shed, PA* (Unpublished master's thesis). University of Delaware, Newark, DE.
785 Merritts, D., Walter, R., Rahnis, M., Cox, S., Hartranft, J., Scheid, C., ... Kather-
786 ine, D. (2013). The rise and fall of Mid-Atlantic streams: Millpond sedi-
787 mentation, milldam breaching, channel incision, and stream bank erosion.
788 In J. V. De Graff & J. E. Evans (Eds.), *The challenges of dam removal and*
789 *river restoration* (21st ed., pp. 183–203). Boulder, CO: Geological Society of
790 America. doi: 10.1130/2013.4121(14)
791 Merritts, D., Walter, R., Rahnis, M., Hartranft, J., Cox, S., Gellis, A., ... Winter,
792 A. (2011). Anthropocene streams and base-level controls from historic dams
793 in the unglaciated mid-Atlantic region, USA. *Philosophical Transactions of the*
794 *Royal Society A: Mathematical, Physical and Engineering Sciences*, *369*(1938),
795 976–1009. doi: 10.1098/rsta.2010.0335
796 Millar, R. G., & Quick, M. C. (1993). Effect of bank stability on geometry of gravel
797 rivers. *Journal of Hydraulic Engineering*, *119*(12), 1343–1363. doi: 10.1061/
798 (ASCE)0733-9429(1993)119:12(1343)
799 Millar, R. G., & Quick, M. C. (1998). Stable width and depth of gravel-bed rivers
800 with cohesive banks. *Journal of Hydraulic Engineering*, *124*(10), 1005–1013.
801 doi: 10.1061/(ASCE)0733-9429(1998)124:10(1005)
802 Parker, G. (1978). Self-formed straight rivers with equilibrium banks and mobile
803 bed. part 2. the gravel river. *Journal of Fluid Mechanics*, *89*(1), 127–146. doi:
804 10.1017/S0022112078002505
805 Parker, G. (1990). Surface-based bedload transport relation for gravel rivers. *Journal*
806 *of hydraulic research*, *28*(4), 417–436. doi: 10.1080/00221689009499058
807 Parker, G. (1991). Selective sorting and abrasion of river gravel. i: The-
808 ory. *Journal of Hydraulic Engineering*, *117*(2), 131–147. doi: 10.1061/
809 (ASCE)0733-9429(1991)117:2(131)
810 Parker, G. (2008). Transport of gravel and sediment mixtures. In M. Garcia (Ed.),
811 *Sedimentation engineering: Processes, measurements, modeling, and practice*
812 (pp. 165–251). Reston, VA: American Society of Civil Engineers.
813 Parker, G., & Klingeman, P. C. (1982). On why gravel rivers are paved. *Water Re-*
814 *sources Research*, *18*(5), 1409–1423. doi: 10.1029/WR018i005p01409
815 Parker, G., Klingeman, P. C., & McLean, D. G. (1982). Bedload and size distribu-
816 tion in paved gravel-bed streams. *Journal of the Hydraulics Division, ASCE*,
817 *108*(HY4), 544–571.

Pazzaglia, F. J. (1993). Stratigraphy, petrography, and correlation of late Cenozoic middle Atlantic Coastal Plain deposits: Implications for late-stage passive-margin geologic evolution. *Geological Society of America Bulletin*, *105*(12), 1617–1634. doi: 10.1130/0016-7606(1993)105⟨1617:SPACOL⟩2.3.CO;2

Pearson, A. J., & Pizzuto, J. (2015). Bedload transport over run-of-river dams, Delaware, USA. *Geomorphology*, *248*, 382–395. doi: 10.1016/j.geomorph.2015.07.025

Phillips, C. B., & Jerolmack, D. J. (2014). Dynamics and mechanics of bedload-tracer particles. *Earth Surface Dynamics*, *2*(2), 513–530. doi: 10.5194/esurf-2-513-2014

Phillips, C. B., & Jerolmack, D. J. (2019). Bankfull transport capacity and the threshold of motion in coarse-grained rivers. *Water Resources Research*, *55*(2), 11316-11330. doi: 10.1029/2019WR025455

Pico, T., Mitrovica, J. X., Perron, J. T., Ferrier, K. L., & Braun, J. (2019). Influence of glacial isostatic adjustment on river evolution along the US mid-Atlantic coast. *Earth and Planetary Science Letters*, *522*, 176–185. doi: 10.1016/j.epsl.2019.06.026

Pizzuto, J. E., & Meckelnburg, T. S. (1989). Evaluation of a linear bank erosion equation. *Water Resources Research*, *25*(5), 1005–1013. doi: 10.1029/WR025i005p01005

Plank, M. O., Schenck, W. S., & Srogi, L. (2000). *Bedrock geology of the Piedmont of Delaware and adjacent Pennsylvania* (No. 59). Newark, DE: Delaware Geological Survey.

Ramsey, K. W. (2005). *Geology of the Old College Formation Along the Fall Zone of Delaware* (No. 69). Newark, DE: Delaware Geological Survey.

Reed, J. C. (1981). Disequilibrium profile of the Potomac River near Washington, DC–A result of lowered base level or Quaternary tectonics along the Fall Line? *Geology*, *9*(10), 445–450. doi: 10.1130/0091-7613(1981)9⟨445:DPOTPR⟩2.0.CO;2

Reitz, M. D., Jerolmack, D. J., Lajeunesse, E., Limare, A., Devauchelle, O., & Métivier, F. (2014). Diffusive evolution of experimental braided rivers. *Physical Review E*, *89*(5), 052809. doi: 10.1103/PhysRevE.89.052809

Renner, G. T. (1927). The physiographic interpretation of the fall line. *Geographical Review*, *17*(2), 278–286.

Reusser, L. J., Bierman, P. R., Pavich, M. J., Zen, E.-a., Larsen, J., & Finkel, R. (2004). Rapid late Pleistocene incision of Atlantic passive-margin river gorges. *Science*, *305*(5683), 499–502. doi: 10.1126/science.1097780

Rhoades, E. L., O'Neal, M. A., & Pizzuto, J. E. (2009). Quantifying bank erosion on the South River from 1937 to 2005, and its importance in assessing Hg contamination. *Applied Geography*, *29*(1), 125–134. doi: 10.1016/j.apgeog.2008.08.005

Rice, S., & Church, M. (1996). Sampling surficial fluvial gravels; the precision of size distribution percentile sediments. *Journal of Sedimentary Research*, *66*(3), 654–665. doi: 10.2110/jsr.66.654

Schenck, W. S., Srogi, L., & Plank, M. O. (2000). *Bedrock Geologic Map of the Piedmont of Delaware and the Adjacent Pennsylvania* (No. 10). Newark, DE: Delaware Geological Survey.

Segura, C., & Pitlick, J. (2015). Coupling fluvial-hydraulic models to predict gravel transport in spatially variable flows. *Journal of Geophysical Research: Earth Surface*, *120*(5), 834–855. doi: 10.1002/2014JF003302

Stotts, S., O'Neal, M., Pizzuto, J., & Hupp, C. (2014). Exposed tree root analysis as a dendrogeomorphic approach to estimating bank retreat at the South River, Virginia. *Geomorphology*, *223*, 10–18. doi: 10.1016/j.geomorph.2014.06.012

Trimble, S. W. (1981). Changes in sediment storage in the Coon Creek basin, Driftless Area, Wisconsin, 1853 to 1975. *Science*, *214*(4517), 181–183. doi: 10.1126/

science.214.4517.181

Vigilar, G. G., & Diplas, P. (1997). Stable channels with mobile bed: formulation and numerical solution. *Journal of Hydraulic Engineering*, *123*(3), 189–199. doi: 10.1061/(ASCE)0733-9429(1997)123:3(189)

Walter, R. C., & Merritts, D. J. (2008). Natural streams and the legacy of water-powered mills. *Science*, *319*(5861), 299–304. doi: 10.1126/science.1151716

Wilcock, P. R. (1993). Critical shear stress of natural sediments. *Journal of Hydraulic Engineering*, *119*(4), 491–505. doi: 10.1061/(ASCE)0733-9429(1993)119:4(491)

Wilcock, P. R. (2001). Toward a practical method for estimating sediment-transport rates in gravel-bed rivers. *Earth Surface Processes and Landforms*, *26*(13), 1395–1408. doi: 10.1002/esp.301

Wilcock, P. R., & Crowe, J. C. (2003). A surface-based transport model for sand and gravel. *Hydraulic Engineering*, *129*(2), 120. doi: 10.1061/(ASCE)0733-9429(2003)129:2(120)

Wilkinson, B. H., & McElroy, B. J. (2007). The impact of humans on continental erosion and sedimentation. *Geological Society of America Bulletin*, *119*(1–2), 140–156. doi: 10.1130/B25899.1

Wolman, M. G. (1954). A method of sampling coarse river-bed material. *EOS, Transactions American Geophysical Union*, *35*(6), 951–956.

Wolman, M. G. (1955). *The natural channel of Brandywine Creek* (No. 271). Reston, VA: U.S. Geological Survey.

Wolman, M. G. (1967). A cycle of sedimentation and erosion in urban river channels. *Geografiska Annaler: Series A, Physical Geography*, *49*(2-4), 385–395.

Figure 1.

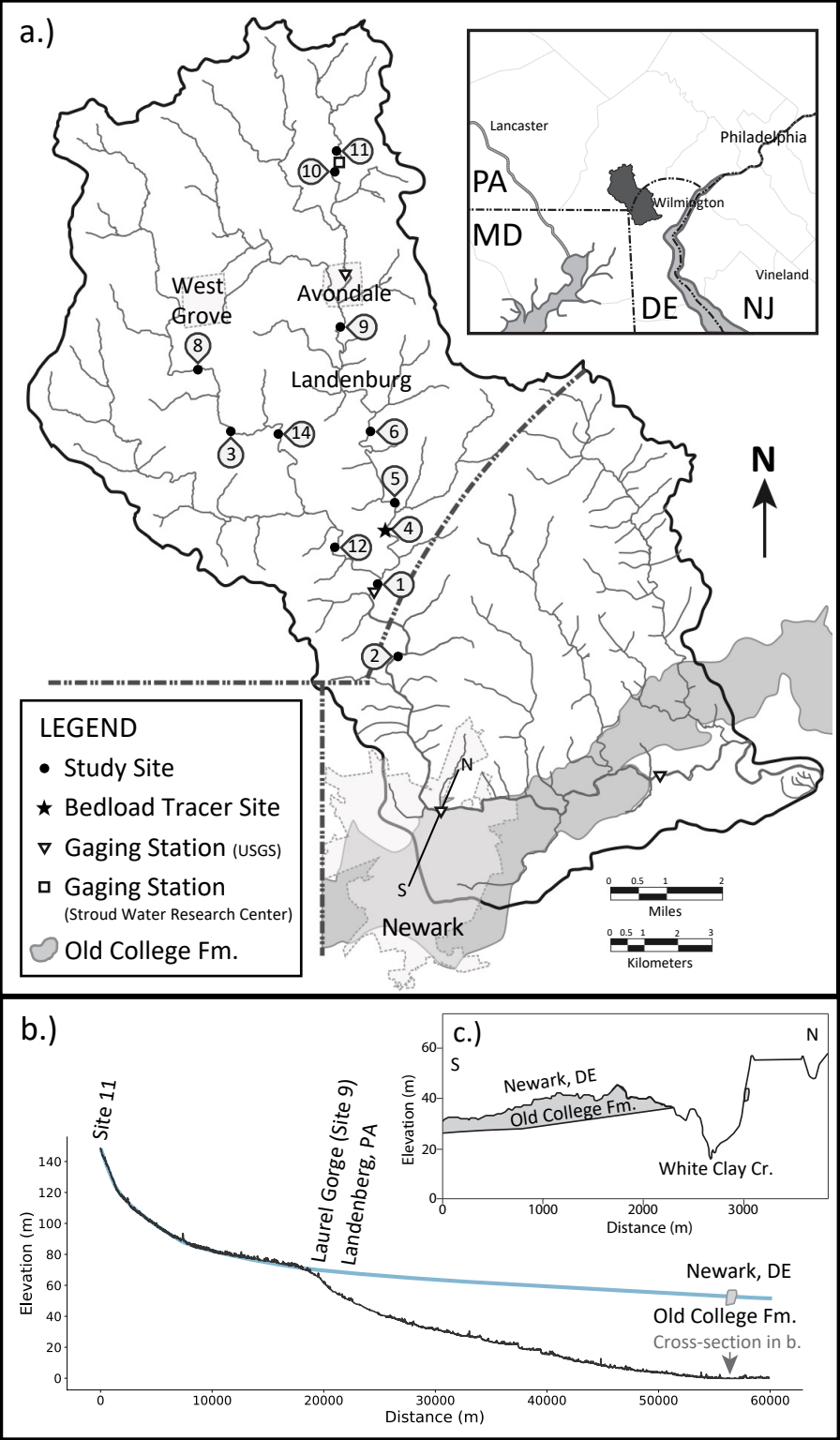
a.)
Lancaster
Philadelphia
PA
Wilmington
MD
Vineland
DE
NJ
West Grove
Avondale
Landenburg
Newark
N
S
LEGEND
Study Site
Bedload Tracer Site
Gaging Station (USGS)
Gaging Station (Stroud Water Research Center)
Old College Fm.
Miles
Kilometers
b.)
Site 11
Laurel Gorge (Site 9) Landenberg, PA
Elevation (m)
Distance (m)
Newark, DE
Old College Fm.
Cross-section in b.
c.)
Newark, DE
Old College Fm.
White Clay Cr.
Elevation (m)
Distance (m)

Figure 2.

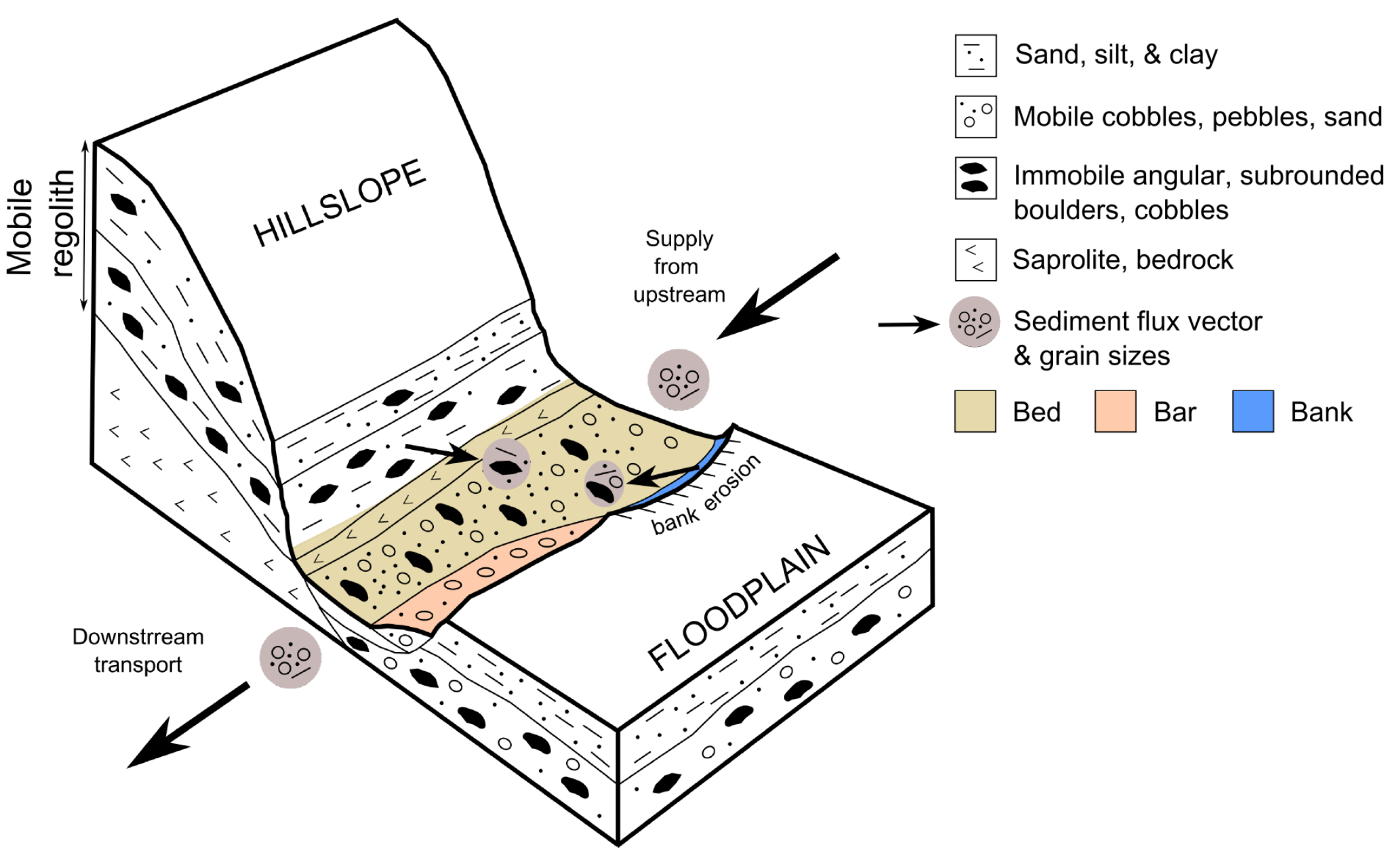
Mobile regolith
HILLSLOPE
Supply from upstream
bank erosion
FLOODPLAIN
Downstrream transport
Sand, silt, & clay
Mobile cobbles, pebbles, sand
Immobile angular, subrounded boulders, cobbles
Saprolite, bedrock
Sediment flux vector & grain sizes
Bed
Bar
Bank

Figure 3.

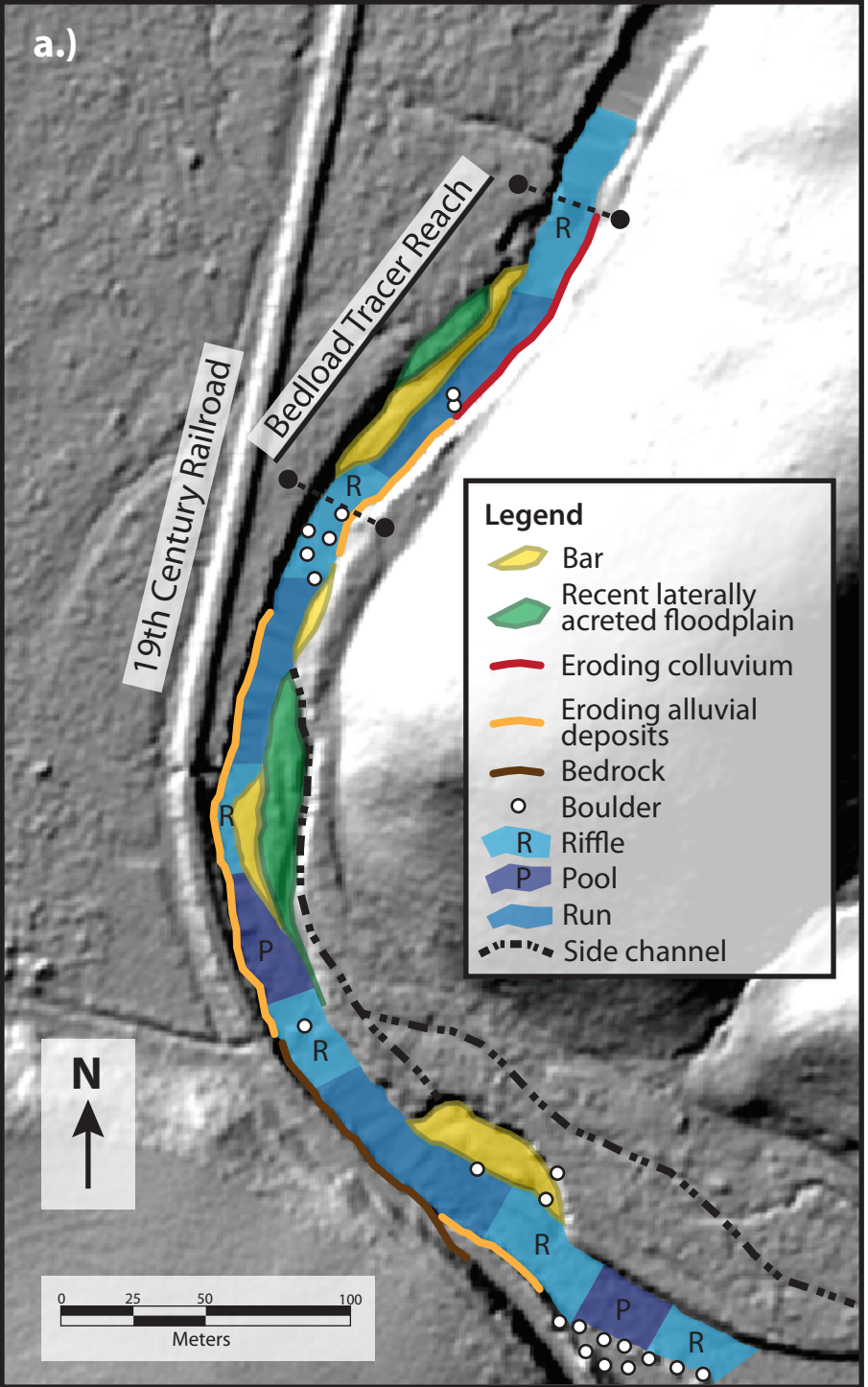
a.)
19th Century Railroad
Bedload Tracer Reach
Legend
Bar
Recent laterally acreted floodplain
Eroding colluvium
Eroding alluvial deposits
Bedrock
Boulder
Riffle
Pool
Run
Side channel
R
P
N
0 25 50 100
Meters

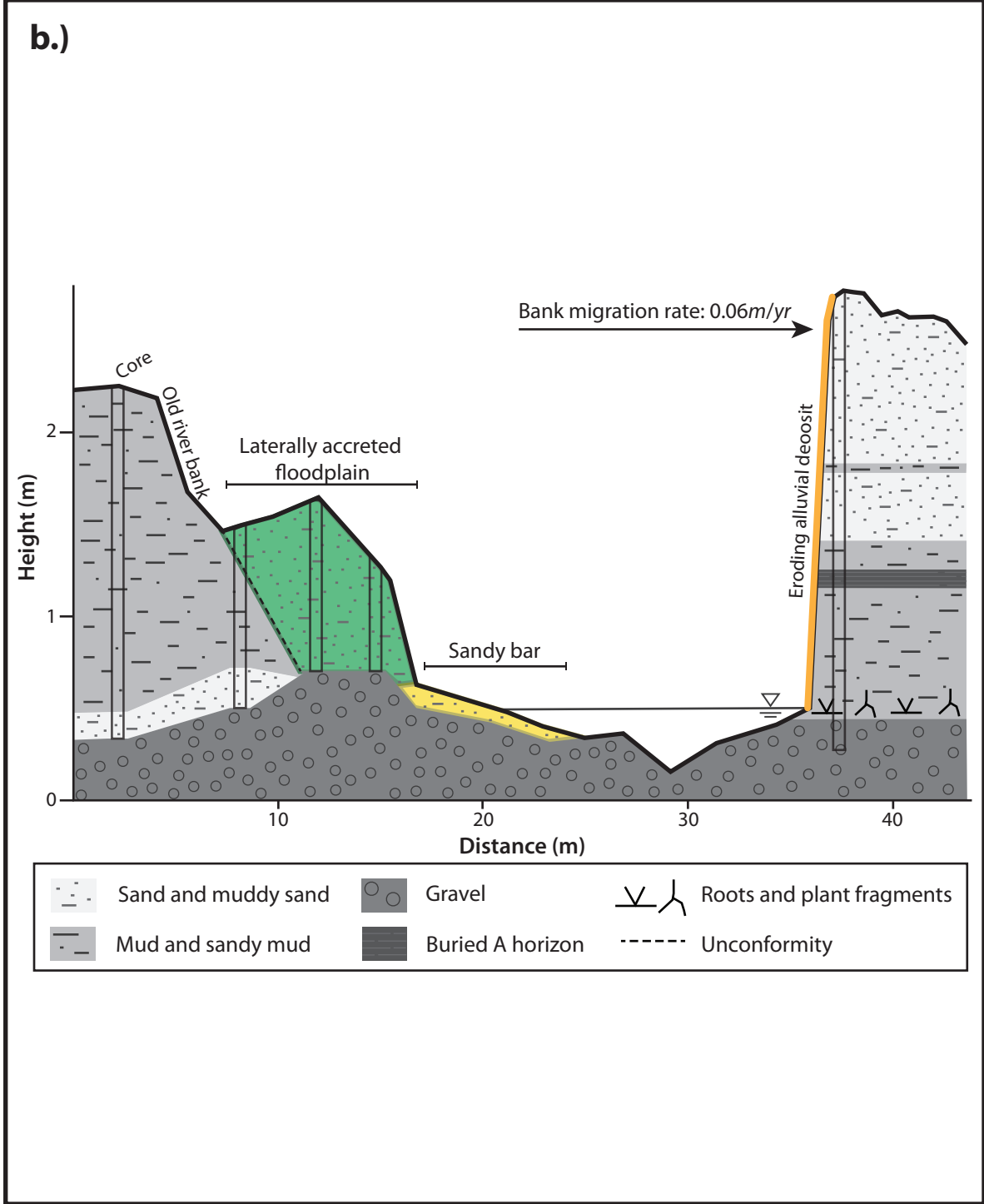
b.)
Bank migration rate: 0.06m/yr
Core
Old river bank
Laterally accreted floodplain
Sandy bar
Eroding alluvial deoosit
Height (m)
0
1
2
10
20
30
40
Distance (m)
Sand and muddy sand
Mud and sandy mud
Gravel
Buried A horizon
Roots and plant fragments
Unconformity

Figure 4.

a.)

Average Bed GSD
Average Bar GSD

Sample Fraction

0.200
0.175
0.150
0.125
0.100
0.075
0.050
0.025
0.000

1-2
2-2.8
2.8-4
4-5.6
5.6-8
8-11
11-16
16-22.6
22.6-32
32-45
45-64
64-90
90-128
128-180
180-256
256-512
512-1024
1024-2048

Grain Size Range (*mm*)

b.)

Cumulative Fraction of Sample

1.0
0.8
0.6
0.4
0.2
0.0

Bed GSD
Average Bed GSD
Bar GSD
Average Bar GSD

10^1
10^2
10^3

Grain Size (*mm*)

Figure 5.

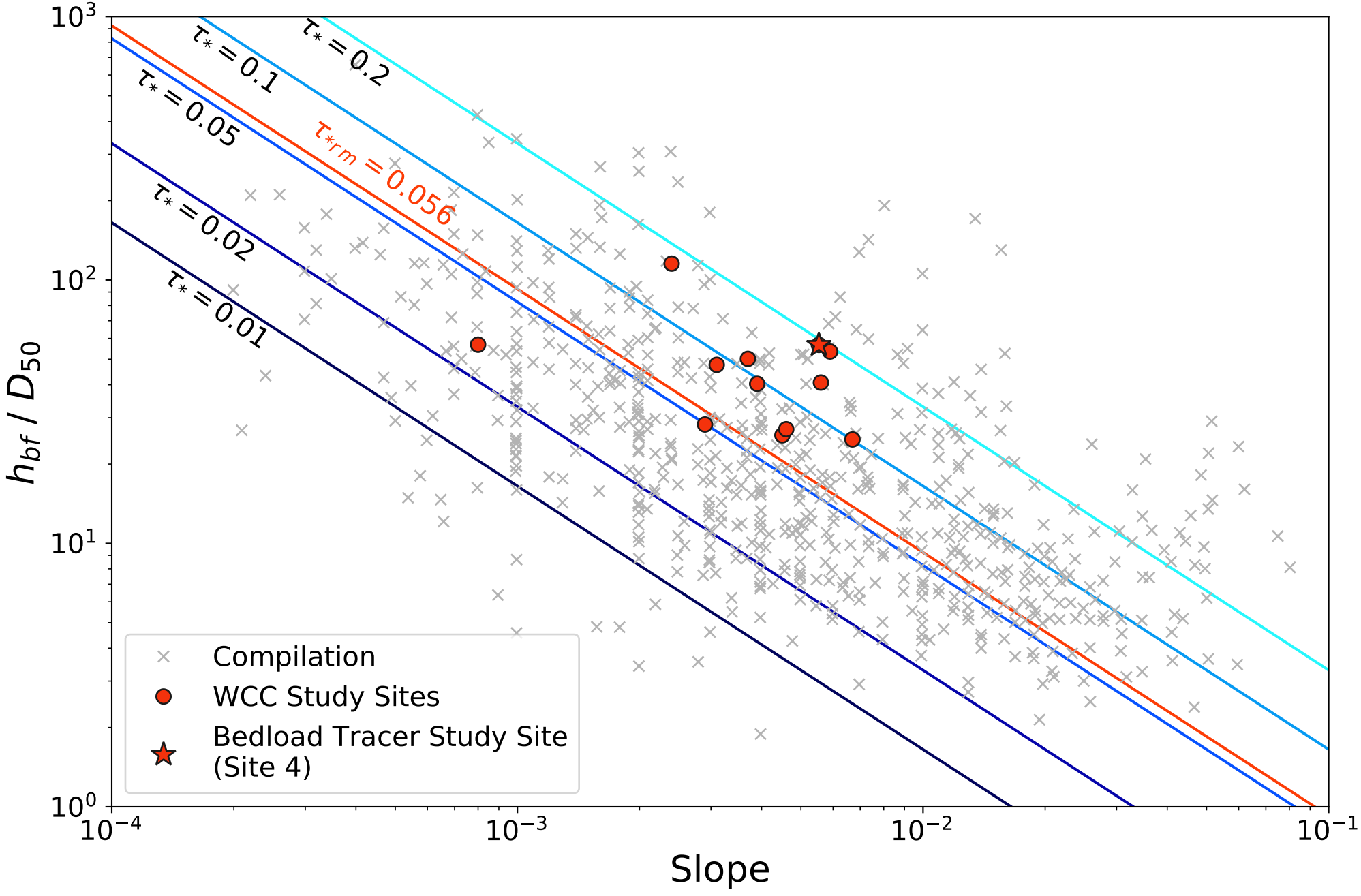
10^3
10^2
10^1
10^0
h_{bf} / D_{50}
10^{-4}
10^{-3}
10^{-2}
10^{-1}
Slope
$\tau_* = 0.2$
$\tau_* = 0.1$
$\tau_* = 0.05$
$\tau_{*rm} = 0.056$
$\tau_* = 0.02$
$\tau_* = 0.01$
Compilation
WCC Study Sites
Bedload Tracer Study Site (Site 4)

Figure 6.

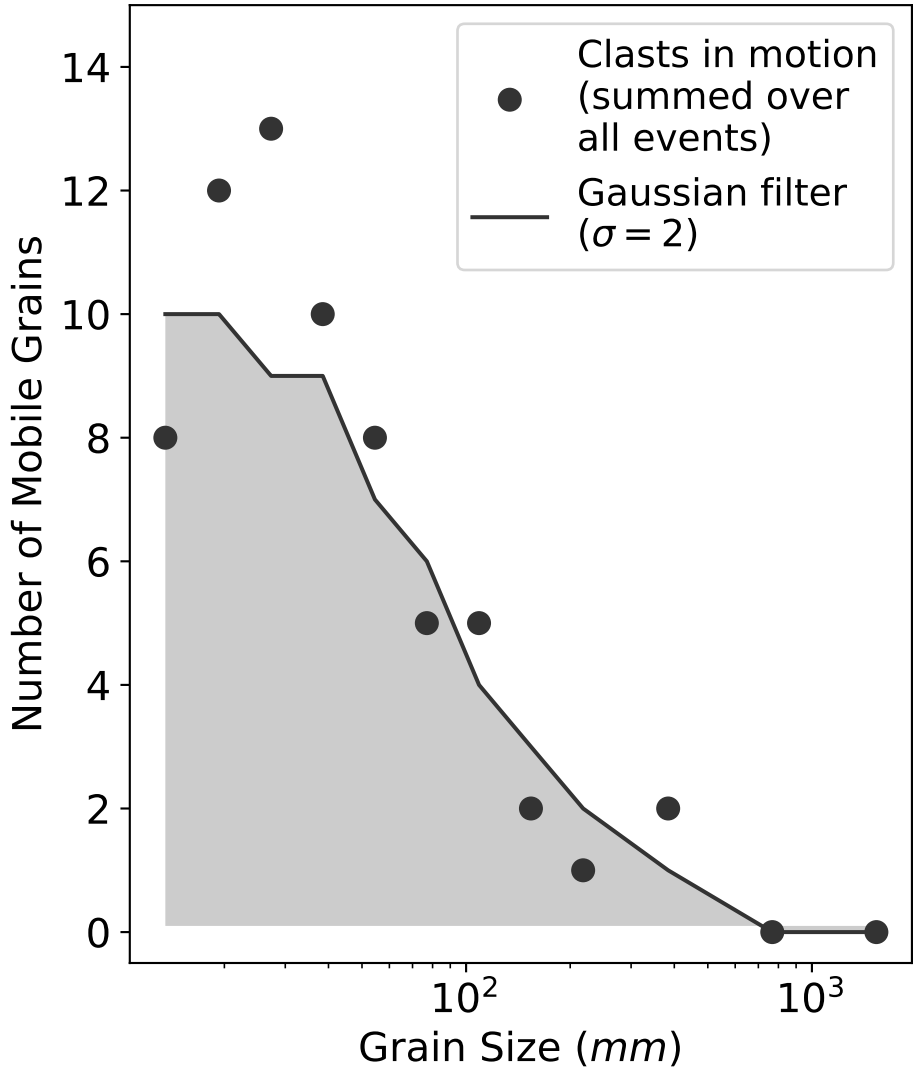
Clasts in motion (summed over all events)
Gaussian filter ($\sigma = 2$)
Number of Mobile Grains
Grain Size (mm)
0
2
4
6
8
10
12
14
10^2
10^3

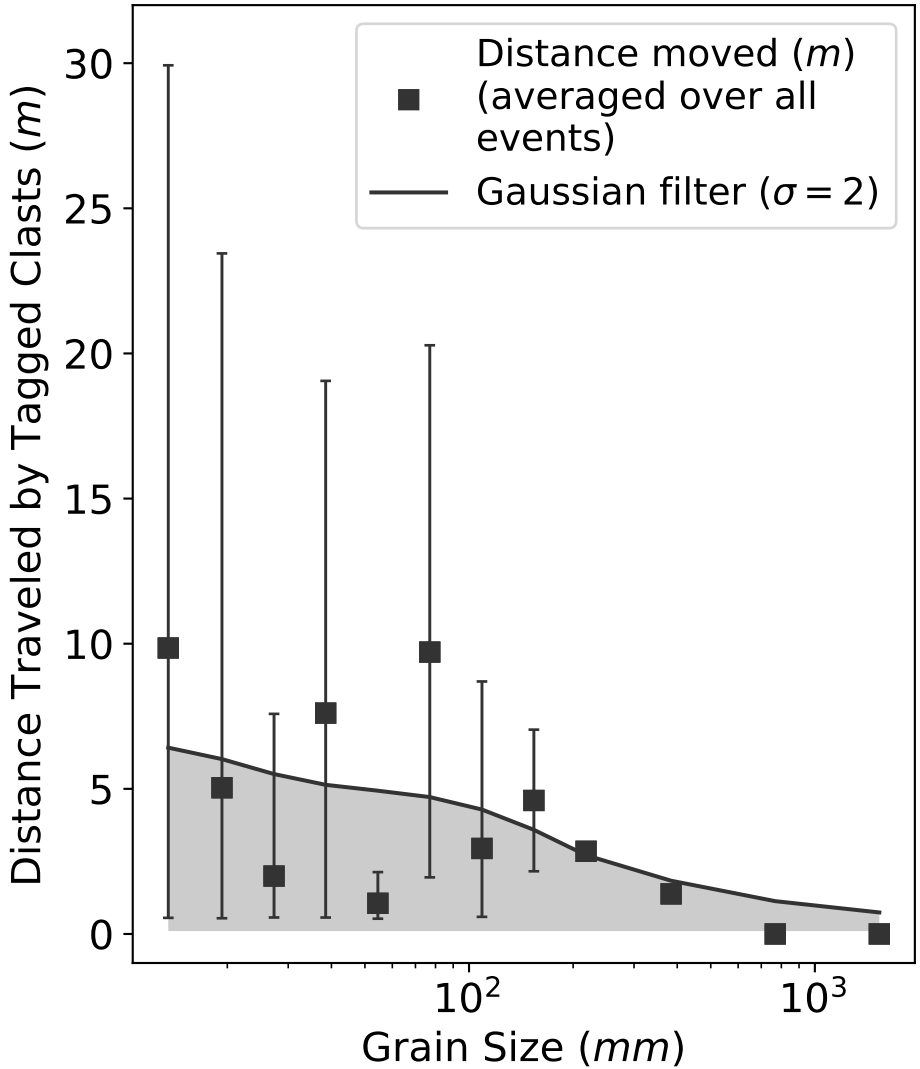
Distance moved (m) (averaged over all events)
Gaussian filter ($\sigma = 2$)
Distance Traveled by Tagged Clasts (m)
Grain Size (mm)
0
5
10
15
20
25
30
10^2
10^3

Figure 7.

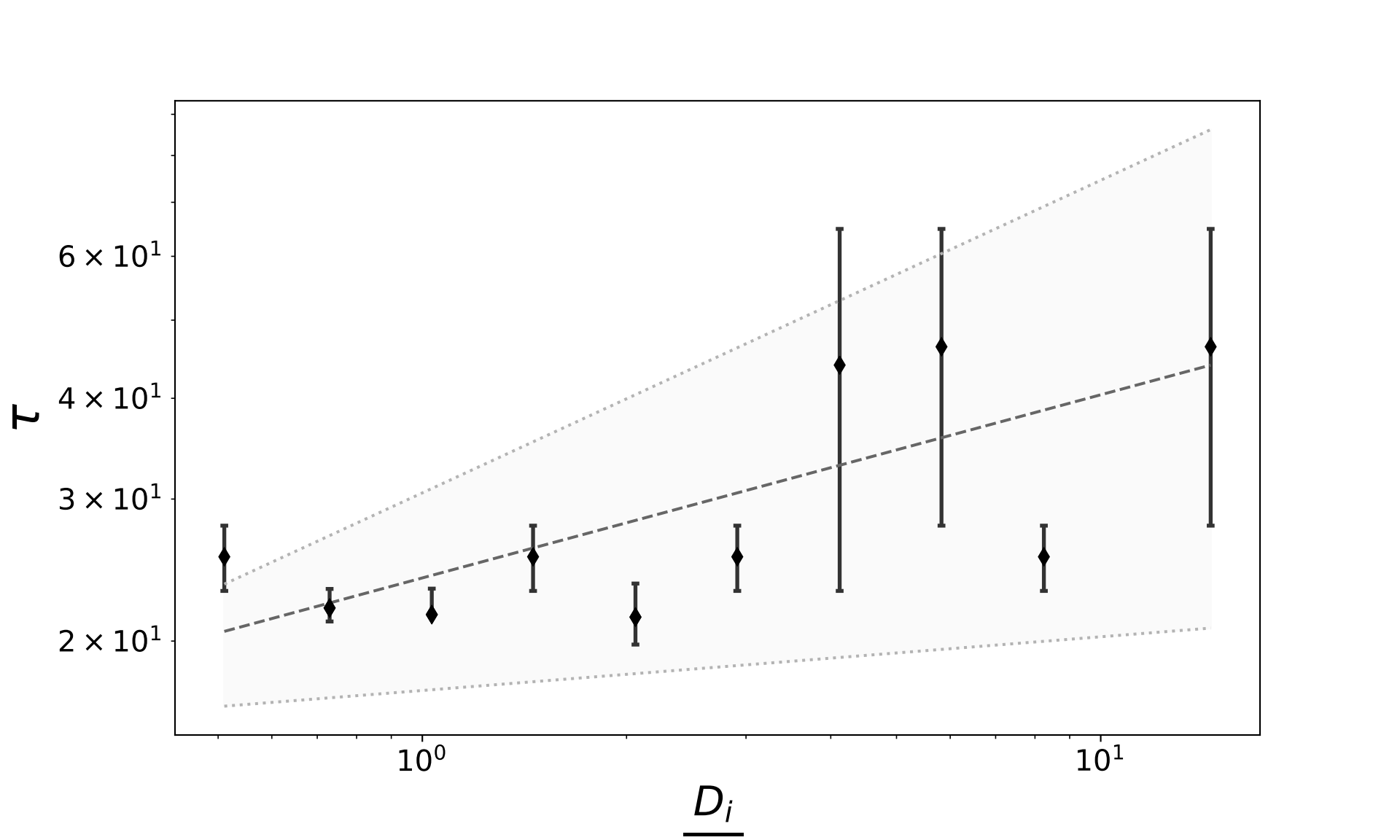
τ
6×10^1
4×10^1
3×10^1
2×10^1
10^0
10^1
$\underline{D_i}$

Figure 8.

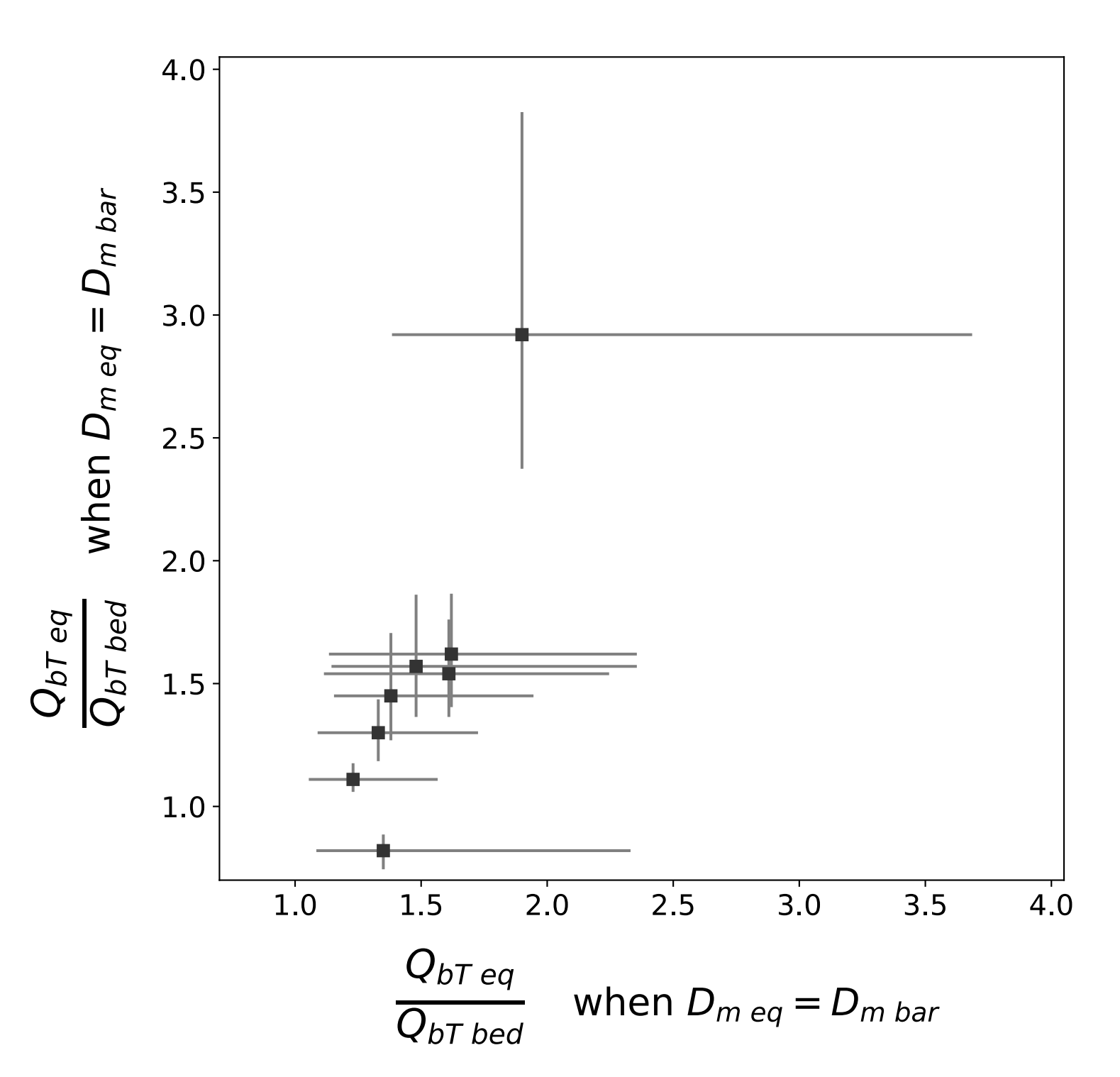
4.0
3.5
3.0
2.5
2.0
1.5
1.0
1.0
1.5
2.0
2.5
3.0
3.5
4.0
$\frac{Q_{bT\ eq}}{Q_{bT\ bed}}$ when $D_{m\ eq} = D_{m\ bar}$
$\frac{Q_{bT\ eq}}{Q_{bT\ bed}}$ when $D_{m\ eq} = D_{m\ bar}$

Figure 9.

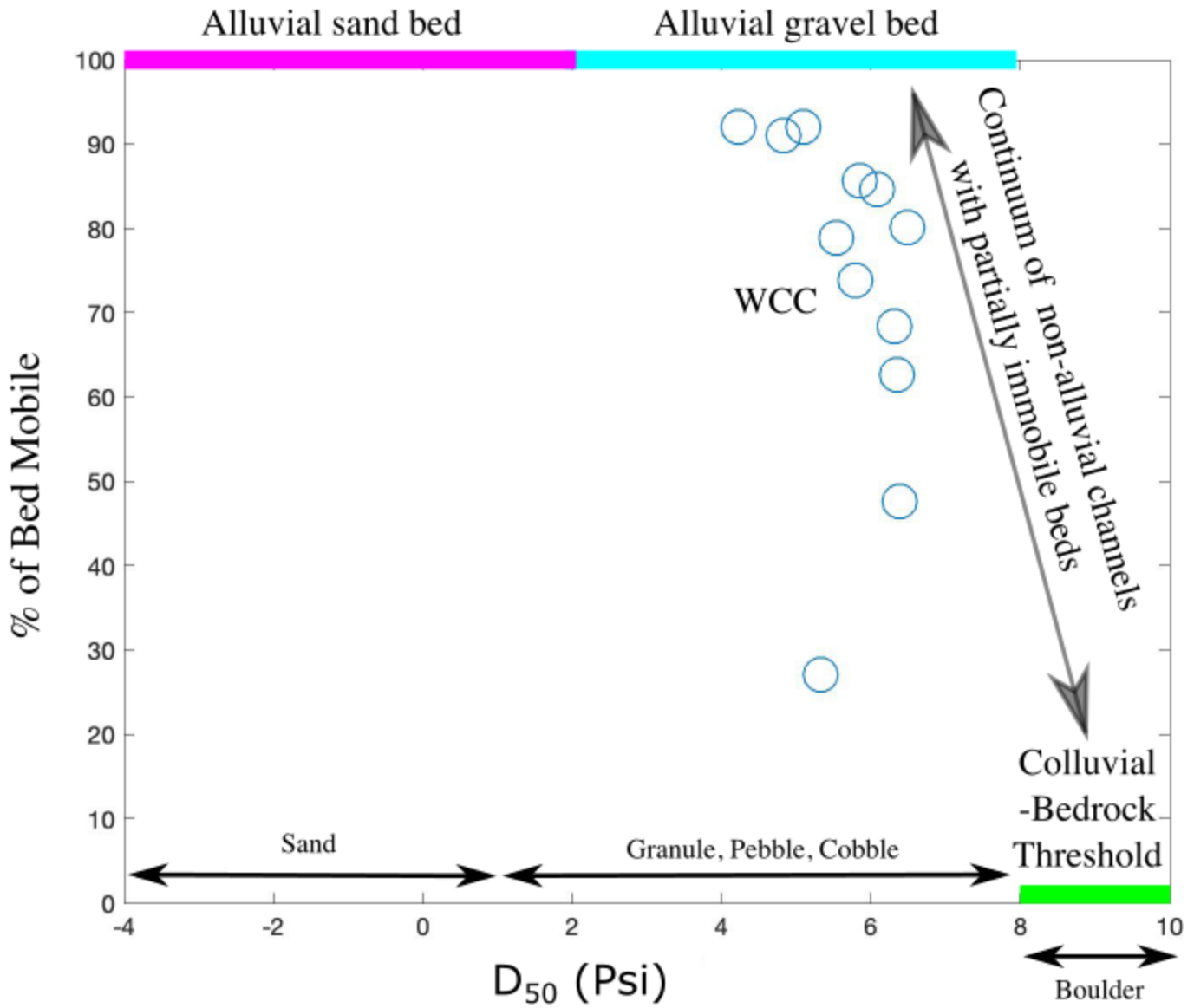
Alluvial sand bed
Alluvial gravel bed
% of Bed Mobile
100
90
80
70
60
50
40
30
20
10
0
-4
-2
0
2
4
6
8
10
WCC
Continuum of non-alluvial channels with partially immobile beds
Colluvial -Bedrock Threshold
Sand
Granule, Pebble, Cobble
Boulder
D50 (Psi)